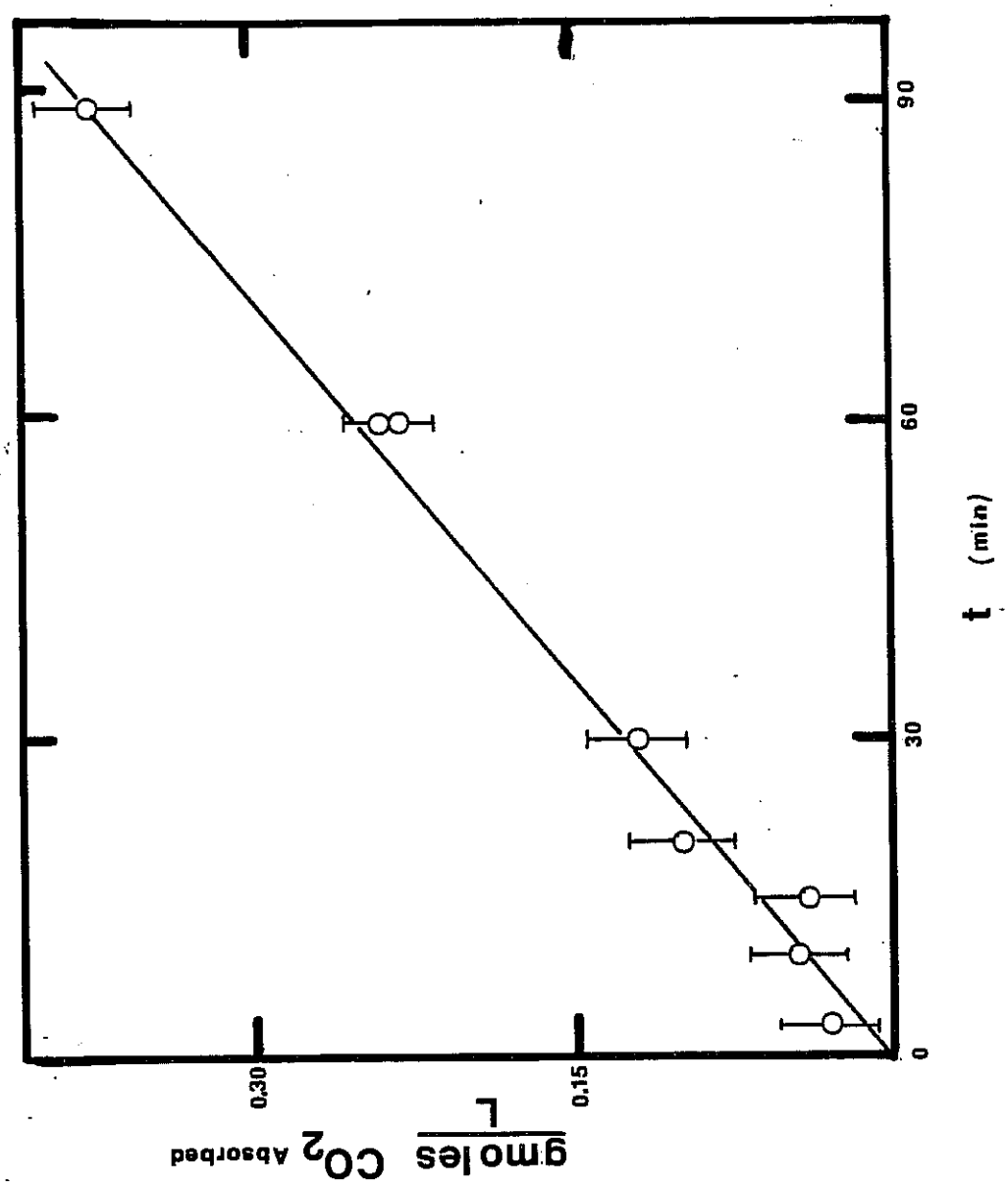

Figure 6. Carbon Dioxide Absorption Versus Time

a more limiting requirement than the requirement to keep the pH and ionic strength constant. Therefore the idea for each run was to get enough change in the bicarbonate concentration to have small titration errors while at the same time limiting the change so that a significant amount of solution was not wasted in diluting it to the next concentration.

3. EQUIPMENT AND PROCEDURE

3.1 EQUIPMENT AND PROCESS FLOW DISCRIPTIONS

Figure 7 is a general schematic for the experimental equipment used in this study. The absorbing solution is pumped from a 15 liter container through 3/4 inch garden hose, a liquid rotameter and two control valves (v1 and v2) to the bottom of the reactor where the gas and liquid initially come into contact. The gas/liquid mixture travels upward through the 1 inch diameter reactor to the separator where the gas and liquid are separated simply by density differences. From the separator, the solution returns through a smaller 1/2 inch tube by gravity flow to the bucket where it is recycled.

The gas rotameters have a maximum capacity of 2.2×10^{-4} m^3/s for nitrogen and 1.6×10^{-4} m^3/s for carbon dioxide. The liquid rotameter has a maximum capacity of 3.2×10^{-4} m^3/s. These capacities translate into the following superficial velocities in the reactor:

V_G from 0.074 to 0.32 m/s; and

V_L from 0.193 to 0.63 m/s.

The calibration charts are given in Appendix 7.3.

The gas, either carbon dioxide or nitrogen, flows from pressurized gas cylinders with regulators through a 1/4 inch gas line, a gas flowmeter with a control valve and a solenoid on/off valve to the bottom of the reactor. The long gas lines before and after the flowmeters have been

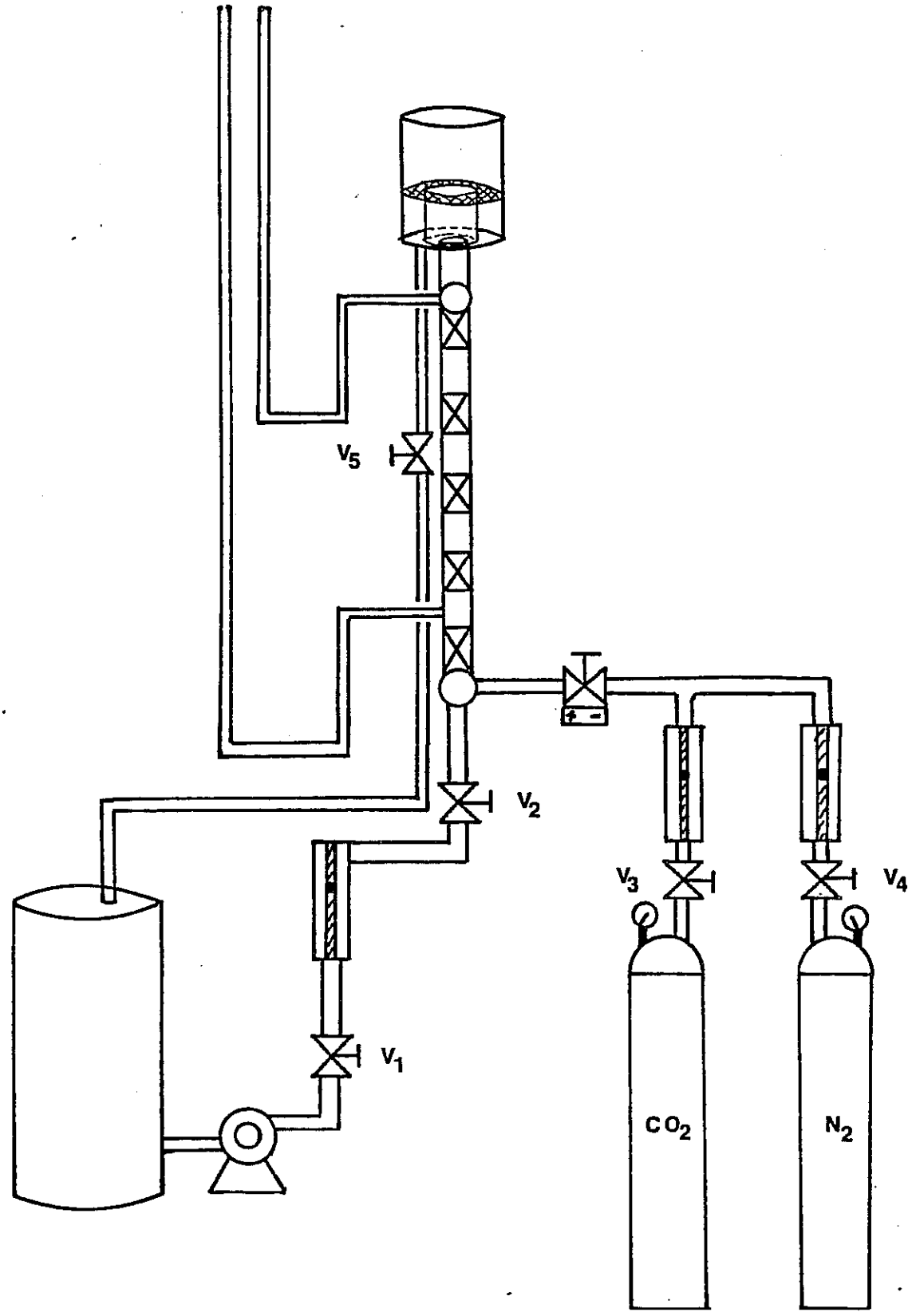

Figure 7. Schematic of the General Equipment

coiled in order to assure the inlet gas to the reactor is at room temperature. From the separator, the gas is released to the atmosphere. The gas solenoid valve and the liquid shut off valve, v2, can be closed quickly and simultaneously for the holdup measurements.

Two 1/4 inch pressure tap lines, one near the bottom of the reactor but still away from the gas inlet and the other at the top of the reactor just below the separator, are connected to two separate water/air manometers used for the total pressure drop measurements.

Figure 8 gives a more complete picture of the pressure drop measurement equipment. It shows that the monometers can be connected to a water supply with a control valve and flowmeter in between. This additional feature was added in order to properly assure that all the pressure lines are constantly filled with water by supplying a small water purge stream. For the pressure measurements for the Koch mixer, the water manometers were substituted by an accurate Helicoid pressure gauge.

Figure 9 shows specifically how the gas is sparged into the liquid mainstream. The gas is injected perpendicularly into the center of the liquid mainstream less than 1 pipe diameter from the first mixing element of the reactor. This method is suggested by the Kenics and Koch Companies.

Figure 10 displays the gas/liquid separator in detail. The separator has a doughnut-shaped wire screen at the top

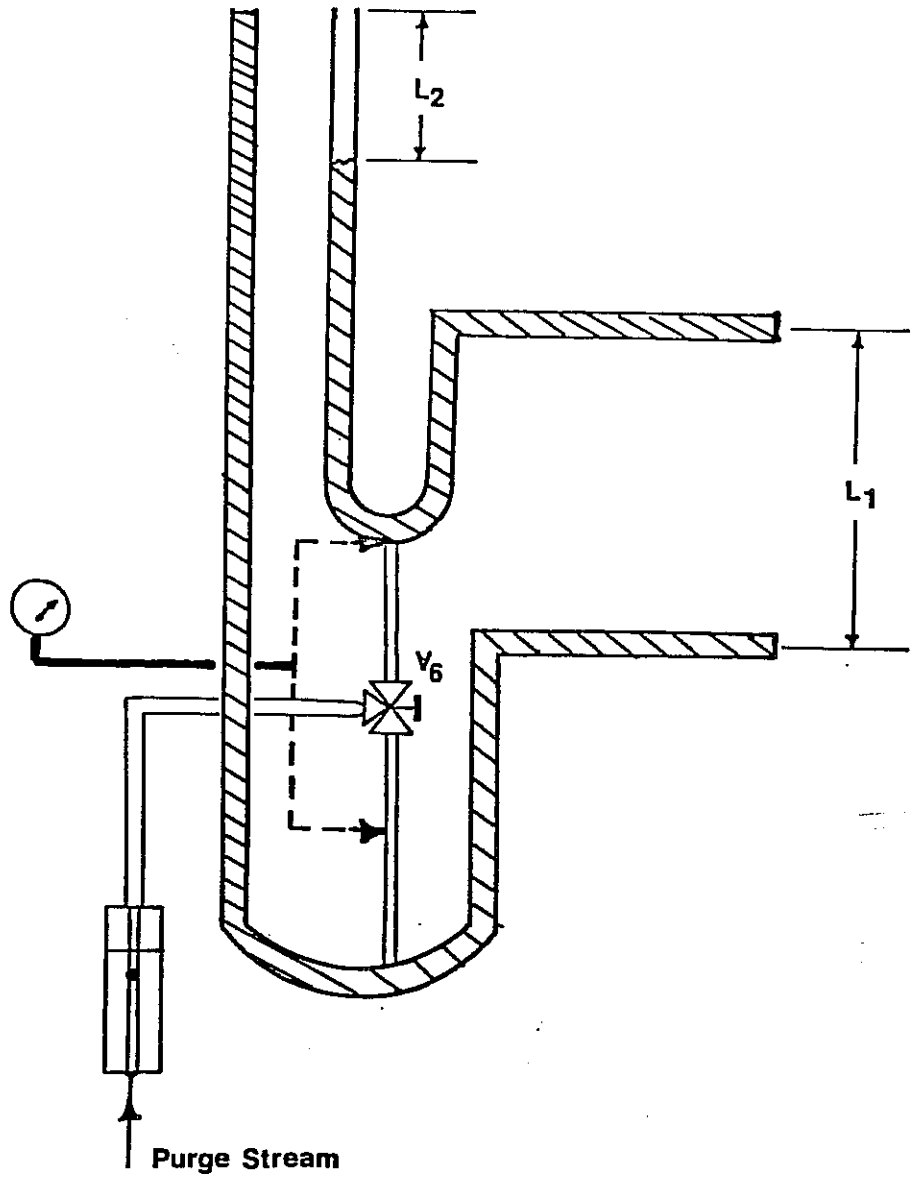

Figure 8. Pressure Measurement Apparatus

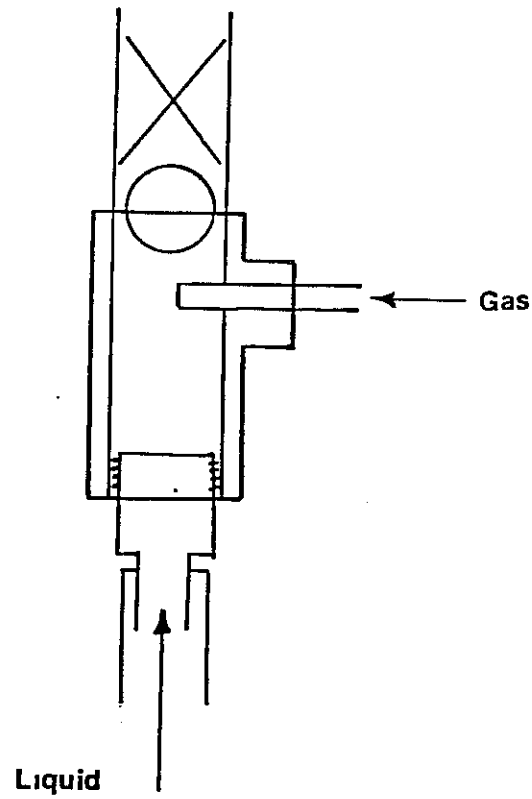

Figure 9. Schematic of Gas Injection into the Liquid Mainstream

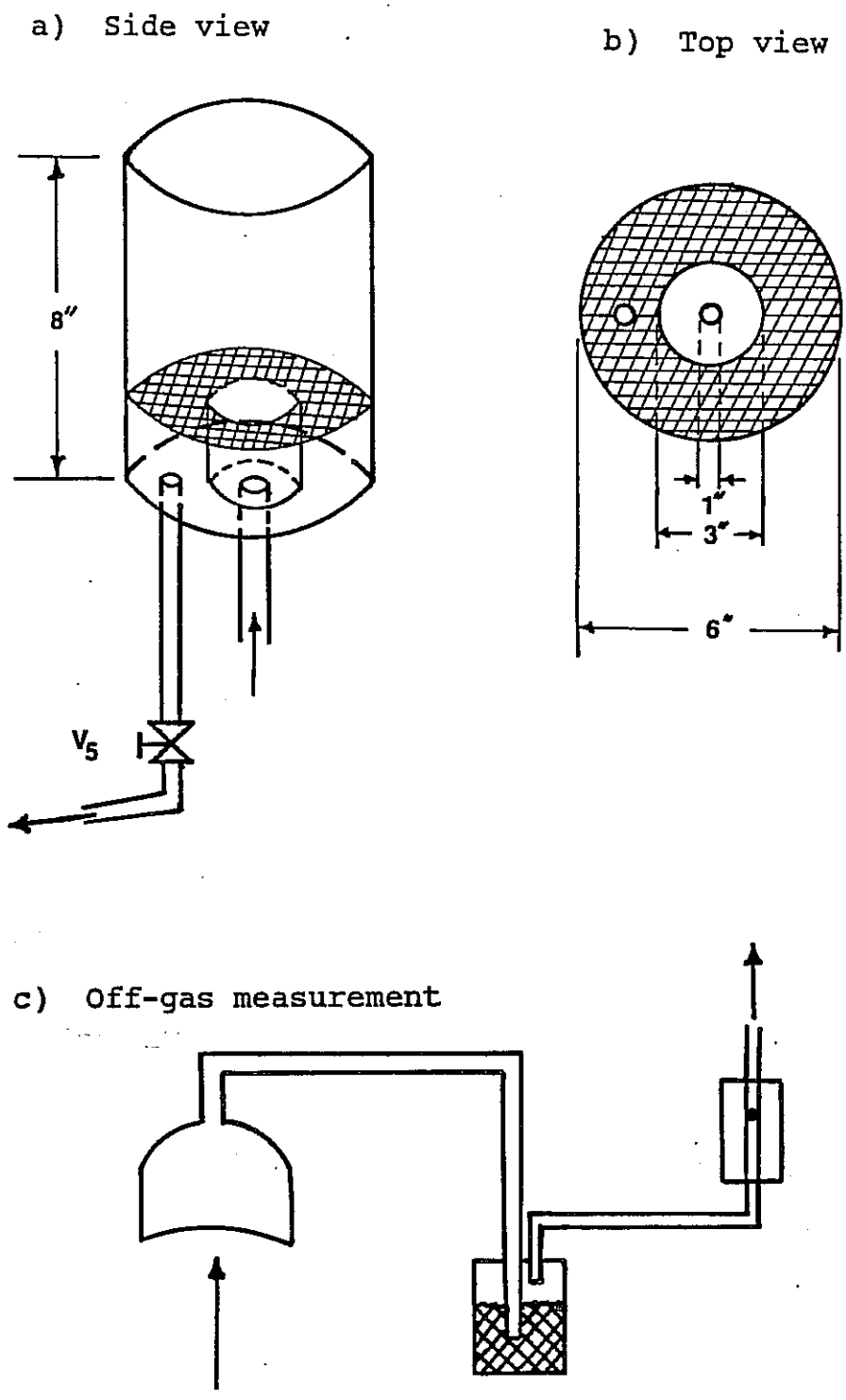

Figure 10. Diagram of the Gas/Liquid Separator

of the liquid outlet to help prevent localized down currents of the liquid that tend to pull gas bubbles down. Valve 5 is simply a pinch valve to control the flowrate out of the separator.

The separator can be fitted with a air tight top in order to capture the off gas, if desired. Experimental problems measuring the off gas flowrate occured with this design. The gas flows from a six inch diameter separator to a 1/4 inch tubing to the outlet flowmeter. Any fluctuation in the liquid rate, changes the liquid height in the separator which causes tremendous fluctuations in the outlet gas flowrate measurement. Also, the outlet gas passes through a water vapor absorption chamber before going to the outlet rotameter. This chamber causes a significant backpressure on the system that affects the sensitivity of the valves. In other words, the backpressure makes it more difficult to maintain steady state in the separator.

Figure 11 is a schematic of the electrical set up for the apparatus. The laboratory power source is split into two branches. The first branch is connected to the pump motor through a variac with an on-off switch. The liquid flowrate is adjusted mainly by this variac, and secondarily by the liquid control valve, v1. The second branch is connected to the following:

1) A timer;

2) The gas solenoid on-off valve;

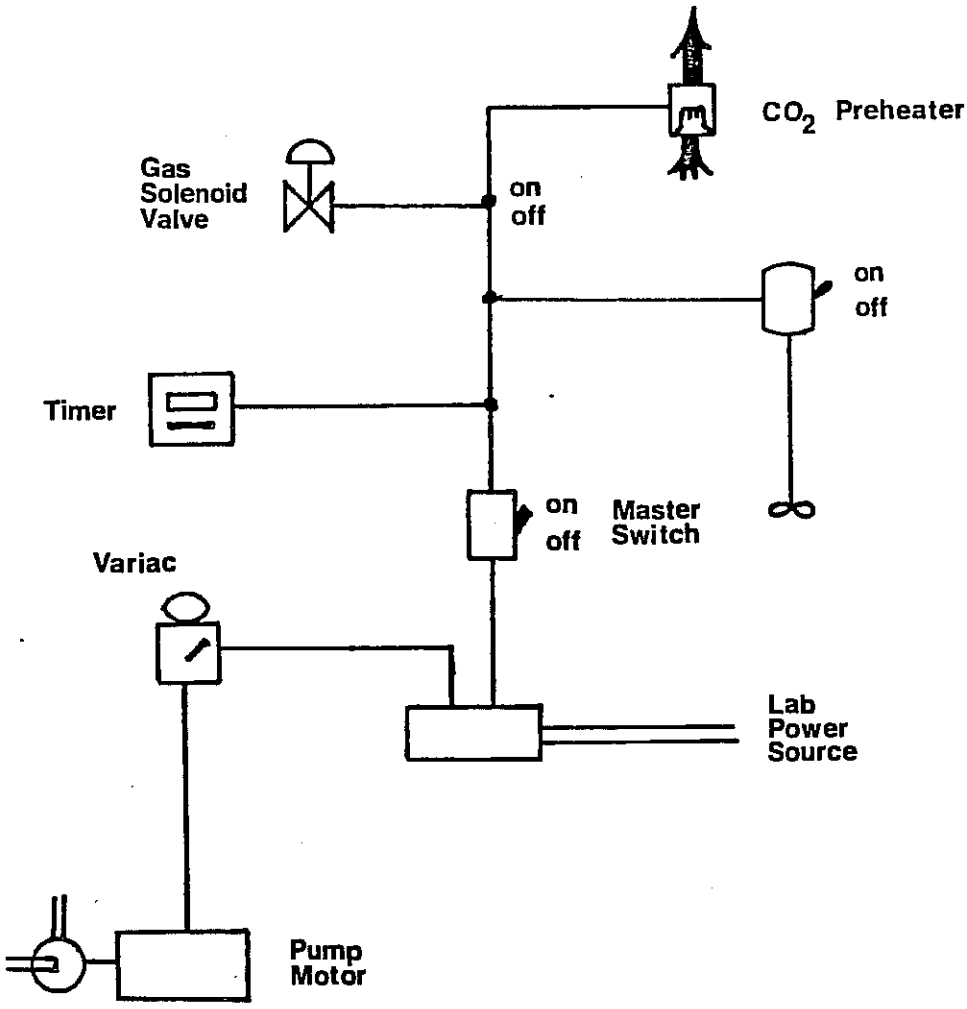

Figure 11. Schematic of the Electrical Connections

3) An electric stirrer to mix solutions in the 15 liter container; and

4) The CO_2 preheater connected between the cylinder and the regulator.

In this configuration, the gas flow can be turned off (by switching the master switch off) without affecting the liquid flow. For holdup measurements the pump can be connected to the second branch in order to stop both flows simultaneously.

The static mixers, in the case of the Kenics and Ross mixers, filled the entire length of the reactor pipe from the gas inlet to the throat of the separator. For the Koch mixer, however, the packing configuration was different. Each Koch segment, which was comprised of two elements rotated 90° to each other, was separated by a spacer of equal length. The spacer was constructed of a thick wire to provide support for the space so that the Koch segments would remain separated even under the highest pressures drops. Since the Koch mixing elements used were significantly denser, this configuration was used in order to obtain the same voidage or the same usable reactor volume per unit length as with the other two mixers.

3.2 EXPERIMENTAL PROCEDURES

The following sections present a general description of the various procedures. Step by step detailed procedures are given in Appendix 7.2.

3.2.1 Holdup and Total Pressure Drop Procedures

The liquid holdup, $1-\epsilon$, and the total pressure drop, ΔP_T, were measured for each reactor type at various gas and liquid flowrates that spanned the capacities of the flowmeters. The procedures to accomplish these measurements are straight forward. Liquid holdup was measured by shuting off the gas and liquid flows into the reactor quickly and simultaneously with the shut-off valves and then measuring the volume of the liquid remaining in the reactor. The liquid holdup was then calculated as the ratio of the volume of liquid remaining and the total volume of liquid the reactor can contain.

The total pressure drop across the column was measured with the use of water manometers or a pressure guage. When carbon dioxide and the buffer solution were used to measure the pressure drop instead of nitrogen and water, the water purge apparatus was used to insure that all the pressure tap lines were filled with only water. With the gas and liquid flowing through the reactor at a constant rate, the total pressure drop is determined from the difference in height of the two water manometers or from the gauge pressure

readings. Refering to Figure 8, the total pressure drop was calculated by one of the following equation:

$$\Delta P_T = (L_1 + L_2)\, g\, \rho_{H_2O} \quad (29)$$

or

$$\Delta P_T = (\Delta P_{guage}) + L_2\, g\, \rho_{H_2O} \quad (30)$$

where L_1 = The liquid level difference of the two manometers, (m); and

L_2 = The height difference of the two pressure taps, (m).

Holdup and pressure drop measurements were performed for nitrogen/water system and for carbon dioxide/buffer system. The two systems gave slightly different results because of their different physical properties and because of the absorption of the carbon dioxide in the latter system. Section 4.1 and 4.2 present the data for the nitrogen/water system while the results by the carbon dioxide/buffer system were used for the absorption calculations and power calculations.

3.2.2 Mass Transfer Procedure

The basic procedure for the evaluation of a and k_L depends on the determination of the rate of absorption of carbon dioxide at various catalyst concentrations. The rate of absorption of carbon dioxide can be directly related to the rate of appearance of bicarbonate in the solution through stoichiometry. The rate of appearance of bicarbonate can be determined by titrating for the bicarbonate

concentration change in the buffer solution after a certain contact time with carbon dioxide gas. Therefore, the basic procedure is to titrate for the bicarbonate concentration change of a solution after a certain reaction time for various solutions of different catalyst concentrations. This procedure is then repeated for various gas and liquid flowrates that span the capacities of the flowmeters and for the three different reactors.

This procedure is complicated by the desire to reuse the solutions in order to reduce the expense of the catalyst. Since, there are no practical separation methods only the operations of dilution and addition of the less costly compounds are available to readjust the concentrations of all species to the desired levels. The required concentrations of all species at the beginning of any run are as follows:

1) The concentration of bicarbonate equals 0.2 M;

2) The concentration of carbonate equals 0.6 M; and

3) The concentrations of catalyst and salt should always be less than or equal to 0.5 M and their sum should always equal 0.5 M.

The readjustment procedure begins after a run is completed. The concentration of bicarbonate is determined by titration. The total solution is then diluted by removing a specific volume of the solution and replacing that volume by water. The quantity of solution to be replaced by water is determined by the amount of dilution

necessary to change the concentration of bicarbonate from the evaluated final concentration of the previous run to 0.2 M. Once the dilution is accomplished the concentrations of the other species have been diminished. The concentration of the catalyst has been reduced which is desired in order to get another point on the Danckwerts' plot. The only thing left to do before starting the new run is to add carbonate in order to get its concentration back up to 0.6 M and to add enough salt in order to reestablish the ionic strength at 2.5.

Figure 12 is a flowsheet that displays a simplified procedure to determine the points necessary for one Danckwerts' plot. The procedure begins by making a buffer solution with the maximum concentration of catalyst and no salt. As the procedure progresses and dilutions are made the concentration of catalyst decreases.

Two major points need to be made concerning this procedure. The first item is that the amount of bicarbonate produced due to the absorption of the carbon dioxide determines the amount of dilution necessary and thereby regulates the next catalyst concentration level. If, for example in the first run in Figure 12, the concentrations after the absorption phase were 0.3 M, 0.55 M and 0.5 M for bicarbonate, carbonate and arsenite, respectively, then the amount of dilution would be 2/3 instead of 1/2 and the final arsenite concentration would be 0.33 M instead of 0.25 M. So by decreasing the absorption time or the amount of carbon

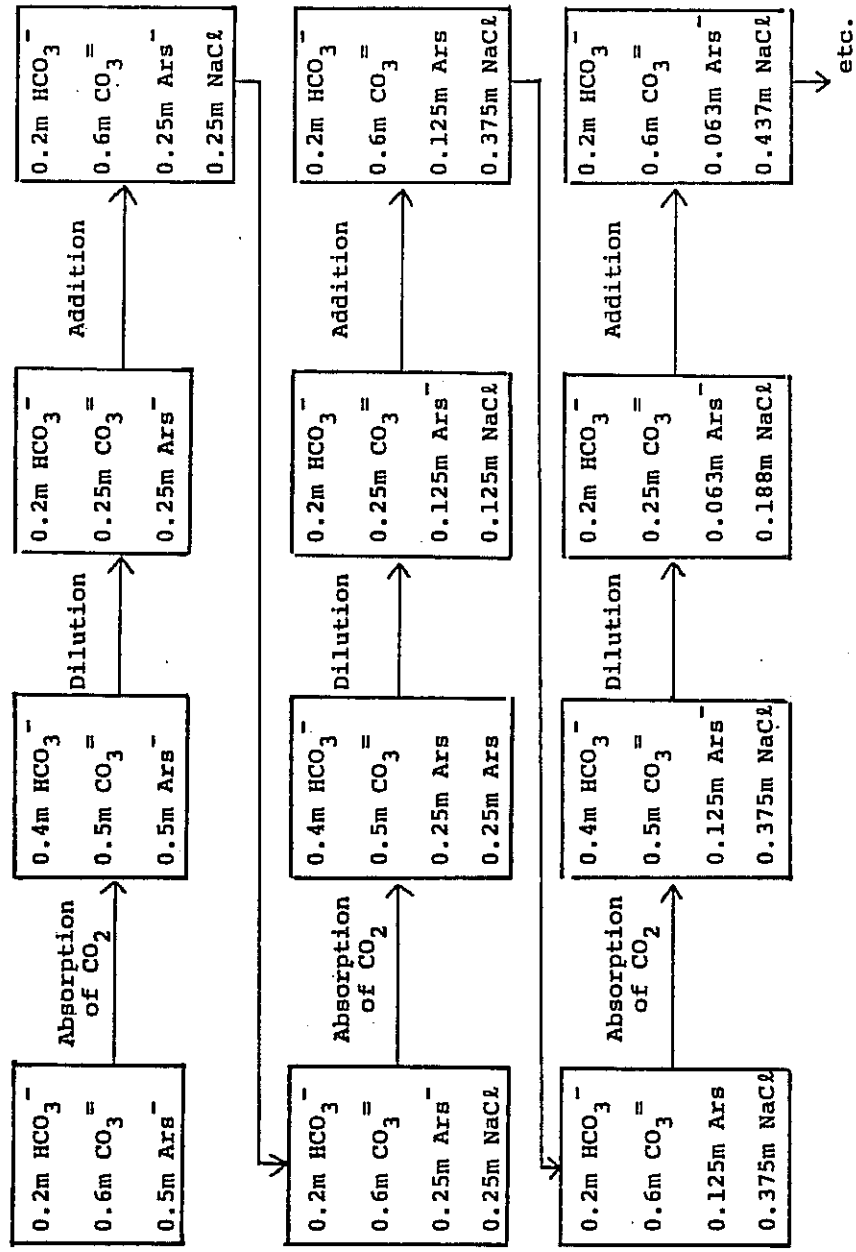

Figure 12. Absorption Procedure Flowsheet

dioxide absorption, more points for one Danckwerts' plot can be obtained. However, since the amount of the absorption is measured by difference the bicarbonate concentrations, the smaller this difference the larger the error for each point. Therefore a trade-off between having many points with large errors for each plot or having a few points with small errors needed to be resolved. It was decided to obtain bicarbonate concentrations of approximately 0.3 M. This gave five to six data points for each Danckwerts' plot with an error of about 15% for each point. The reaction time necessary to obtain this concentration was determined for each run by educated guessing.

The other important point to discuss is the way of keeping track of all the concentrations at the end of every step. This was important because any error would propogate throughout the rest of the procedure.

The tools available to help the bookkeeping of all the concentrations are two different titrations, an accurate balance, the experimentally verified stoichiometry and knowing that there is no depletion of the catalyst during the absorption phase.

The two titrations determine the concentrations of different species. The first titration, which will be refered to as the TBC titration, determines the total base concentration and is extremely accurate and simple. It requires titrating a sample of solution with HCl to a blue to yellow bromophenol blue end point. The second titration,

which determines the concentration of bicarbonate plus the concentration to the catalyst and will be refered to as the BI titration, is difficult and can be accompanied by a significant amount of error. This titration procedure is described fully in Appendix 7.2. So the best overall procedure was to use the TBC titration preferentially over the BI titration.

Refering to Figure 12, bicarbonate and carbonate are accurately weighed and added to pure water in the 15 liter container. Since there may be some water in the process lines, the exact starting volume is unknown. But by using the TBC titration and knowing exactly how much bicarbonate and carbonate is added then the exact volume can be determined. The catalyst can then be added and the TBC titration can be performed again. The difference between the two titrations gives the exact starting concentration of the catalyst. After the absorption, the BI titration must be preformed. The new bicarbonate concentration is now determined by subtracting the known catalyst concentration from the results of this titration. The concentration of carbonate can be evaluated from the stoiciometry. The next step to be performed is the dilution. Once the dilution is performed the exact dilution ratio can be verified by doing th TBC titration and comparing it to the last TBC titration. The knowledge of the exact dilution ratio allows the calculation of all the reduced concentrations. After the dilution, the volume will not exactly be the same as the

original volume due to volumetric measurement errors, so the addition phase can be used to determine the new exact volume by a similar method as the determination of the original volume. This bookkeeping procedure is repeated for each step.

4. RESULTS AND DISCUSSION

4.1 HOLDUP

Liquid holdup, $1-\epsilon$, and gas holdup, ϵ, in a gas/liquid contactor are dependent upon the relative velocities of the gas and liquid phases. For the ideal situation of homogeneous flow, the two phases travel at the same relative velocities or

$$\frac{V_L}{1-\epsilon} = \frac{V_G}{\epsilon} \tag{31}$$

However because of density and viscosity differences, the gas phase often travels faster than the liquid phase and consequently the liquid holdup is larger than it should be ideally. The velocity of the gas relative to the liquid is called the slip velocity, ΔV, and is defined by Wallis (21) in the following equation:

$$\Delta V = \frac{V_G}{\epsilon} - \frac{V_L}{1-\epsilon} \tag{32}$$

Since the two-phase flow is often not homogeneous, some theories and correlations have been developed to predict holdup and other flow parameters. One of the most popular correlations is the Lockhart-Martinelli correlation. For air/water systems, Butterworth (22) gives the following form of this well known correlation:

$$\frac{1-\epsilon}{\epsilon} = 2.4 \left(\frac{V_L}{V_G}\right)^{0.64} \tag{33}$$

Figure 13, 14, 15 show the results of the holdup experiments for the Kenics, Ross, and Koch mixers in a vertical arrangement, respectively, with a nitrogen/water system. Also displayed on these plots for comparison are the homogeneous flow model and the Lockhart-Martinelli correlation. The Kenics and Koch mixer are similar in their plot charateristics. Both mixers have a family of lines of constant liquid superficial velocity that are parallel to and approach the homogeneous flow model line as the liquid superficial velocity increases. This interesting result is contrasted by the characteristics of the plot of the Ross mixer data. Figure 14 shows essentially that all the lines of constant liquid velocity overlap into one line with that line still parallel to the homogeneous line.

Appendix 7.4 analyzes the reason for the differences between the Ross mixer and the other two mixers. Briefly, as the liquid superficial velocity is increased, the slip velocity increases with the Ross mixer but decreases in the case of the Koch and Kenics mixers. This is a revealing difference between the reactor types. The slip velocity will decrease with increased liquid rate if the radial mixing is increased. This is definitely a beneficial characteristic for a static mixer, since increasing the liquid rate is the major way to increasing the turbulence in the mixer.

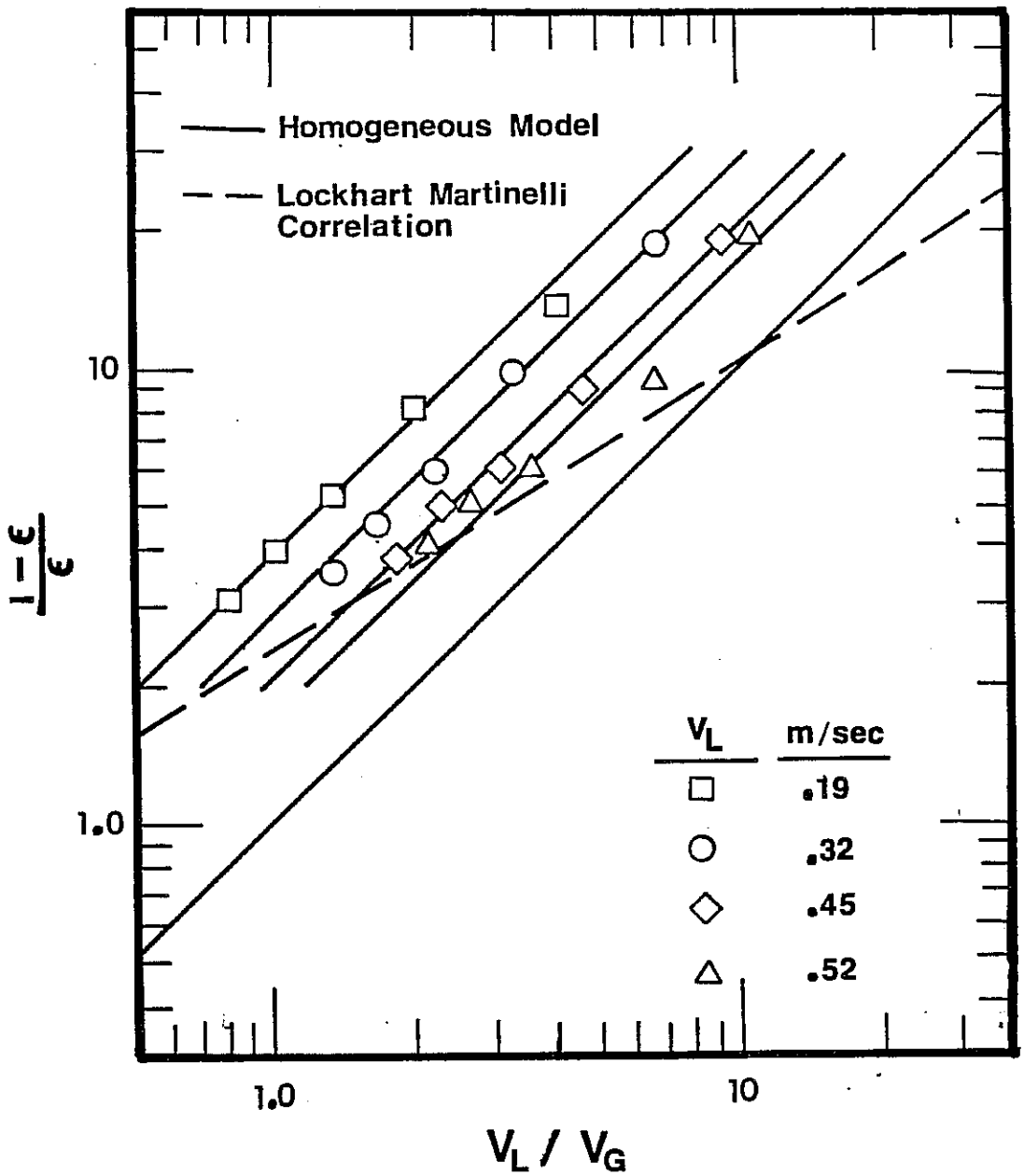

Figure 13. Effect of Fluid Velocity Ratio on the Holdup Ratio in the Kenics Mixer (Vertical)

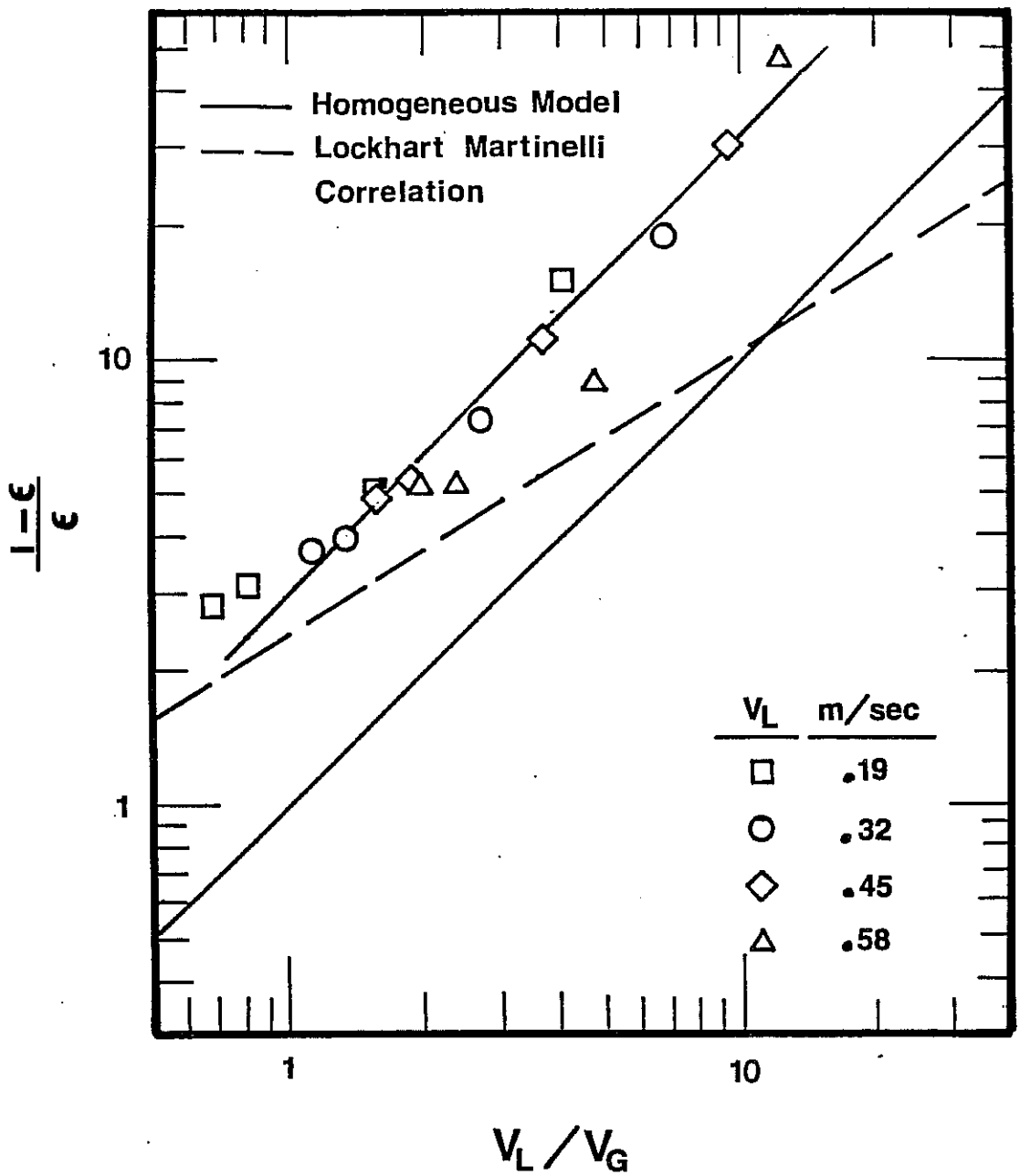

Figure 14. Effect of Fluid Velocity Ratio on the Holdup Ratio in the Ross LLPD Mixer

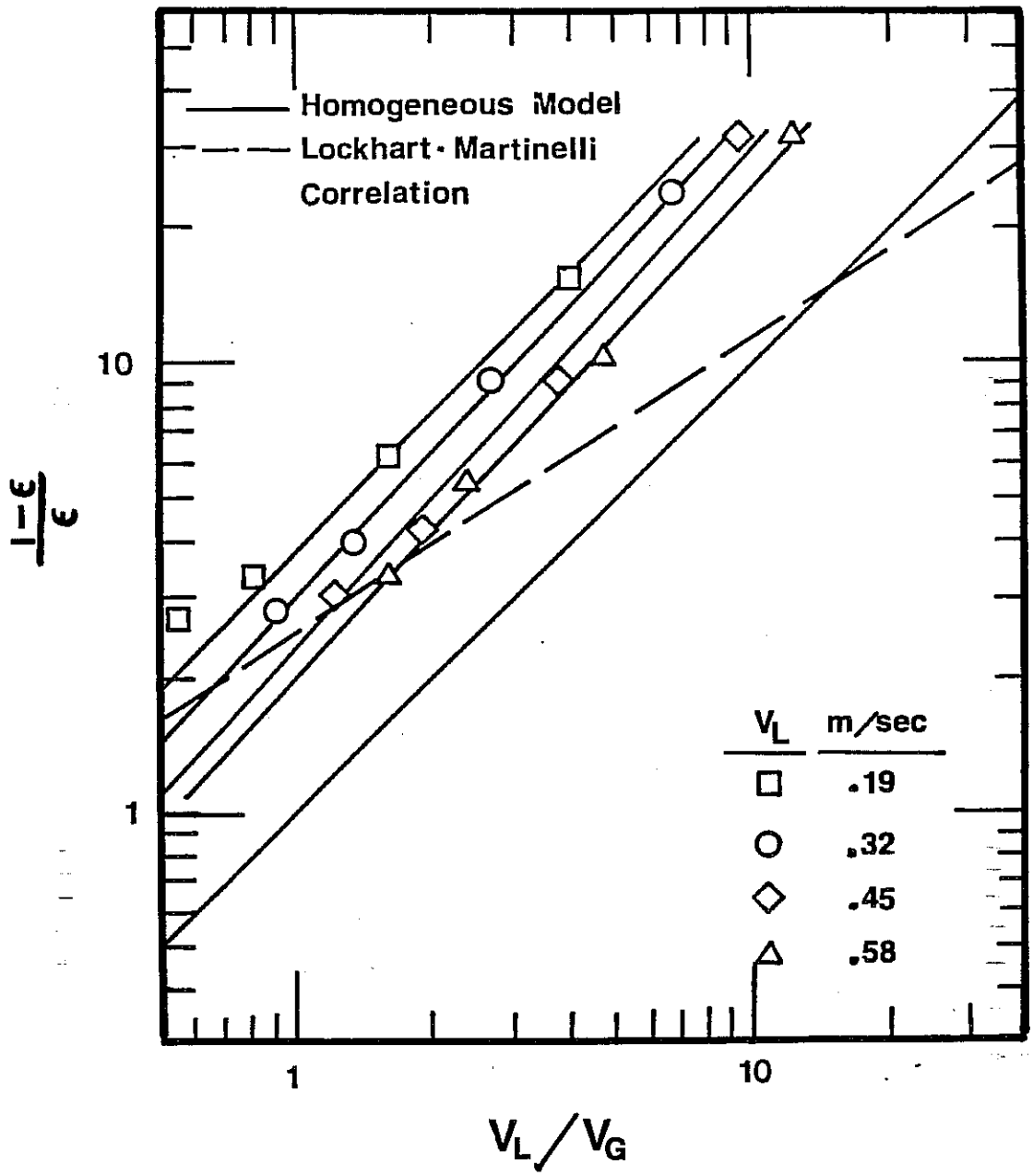

Figure 15. Effect of Fluid Velocity Ratio on the Holdup Ratio in the Koch CY Mixer

The effect of the slip velocity on mass transfer is not as clear cut. Cichy and Russell (23) showed from penetration theory that the liquid side mass transfer coefficient can be estimated from the following equation:

$$k_L = \frac{2}{\sqrt{\pi}} \sqrt{\frac{D_A \, \Delta V}{d_B}} \qquad (6)$$

This equation suggests that the mass transfer is increased by an increase in slip velocity. However, this formula was derived for bubble flow in empty pipes where the shear caused by the velocity differences is a main cause of turbulent effects on the gas/liquid interface. In static mixers, this shear could be insignificant compared to the turbulence induced by the surfaces of the mixer elements.

Horizontal flow in the Kenics mixer is different than upflow. Figure 16 shows that this flow seems to act more like the flow predicted by the Lockhart-Martenilli correlation, although not exactly. Also the family of lines are not as distinct as in the vertical flow. The reason for this difference between vertical and horizontal flow is not immediately clear.

Generally, the gas holdup is larger in the horizontal flow and is caused by the the absence of any static pressure across the reactor. In the vertical flow case, the larger total pressure drop provides a larger driving force in the axial direction which tends to magnify the viscosity and

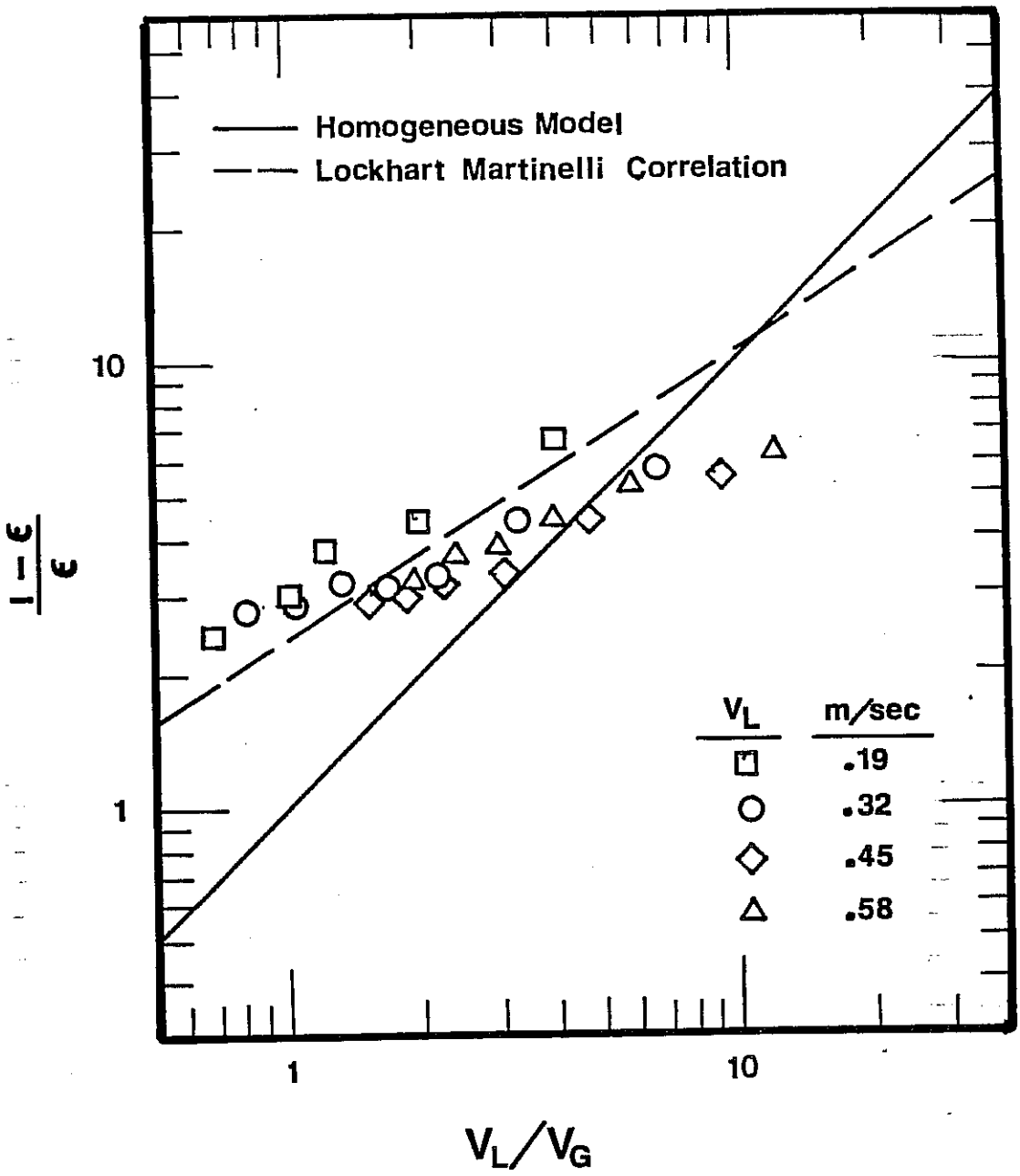

Figure 16. Effect of Fluid Velocity Ratio on the Holdup Ratio in the Kenics Mixer (Horizontal)

density differences of the two fluids. The gas travels faster and consequently the gas holdup decreases in vertical flow.

The family of lines found in Figures 13 and 15 were also seen by Yung Hsu in his investigation of the gas-lift reactor (24). In his doctoral thesis, he suggested a revised model described by the following equation:

$$\frac{1-\epsilon}{\epsilon} = D \left(\frac{V_L}{V_G}\right)^m \qquad (34)$$

where $D = f(V_L, \rho_L, \mu_L, \sigma \ldots)$

He also showed that D1 can be correlated with the two phase Reynolds, Froude, and Weber numbers. It is possible that this type of correlation could be beneficial when discussing the holdups for co-current gas/liquid upflow in the Koch and Kenics mixers. Appendix 7.8 gives this correlation attempt.

4.2 PRESSURE DROP

The accurate prediction of pressure drop across a gas/liquid reactor is essential for the proper design and selection of a suitable in-line mixer. Each commercial static mixer studied has a method to predict the kinetic pressure drop of two phase flow per unit length of the reactor. These methods are all based on the Lockhart-Martinelli correlations, which were derived from the results of two-phase horizontal flow experiments. Based on the evidence in the last section, this method does not necessarily apply when considering upflow. This statement is

substantiated by a study done by John Smith (2), who studied holdup and pressure drops in two phase co-current vertical pipes filled with Kenics mixer. He found "that over the whole range of these experiments the relative increase in pressure drop in the two-phase system is about half that which would be expected in a horizontal straight pipe", as predicted by the Lockhart-Martinelli correlation.

From the last section, the vertical flow is more closely related to the homogeneous flow model although not too closely. The kinetic pressure drop using the homogeneous model can be predicted from the following equation:

$$\frac{\Delta P_K}{L} = \frac{4\ f_H}{2\ d}\ \rho_H\ V_H^{\ 2} \qquad (35)$$

where f_H = Homogeneous friction factor;
V_H = Velocity of homogeneous fluid; and
ρ_H = Density of homogeneous fluid.

The homogeneous velocity can be closely approximated by the liquid superficial velocity and for a constant gas flowrate the homogeneous density can be considered fairly constant. Considering these two approximations, a plot of kinetic pressure drop per unit reactor length versus liquid velocity on log-log paper should give some information in a concise manner. Figure 17 provides this plot using data from the

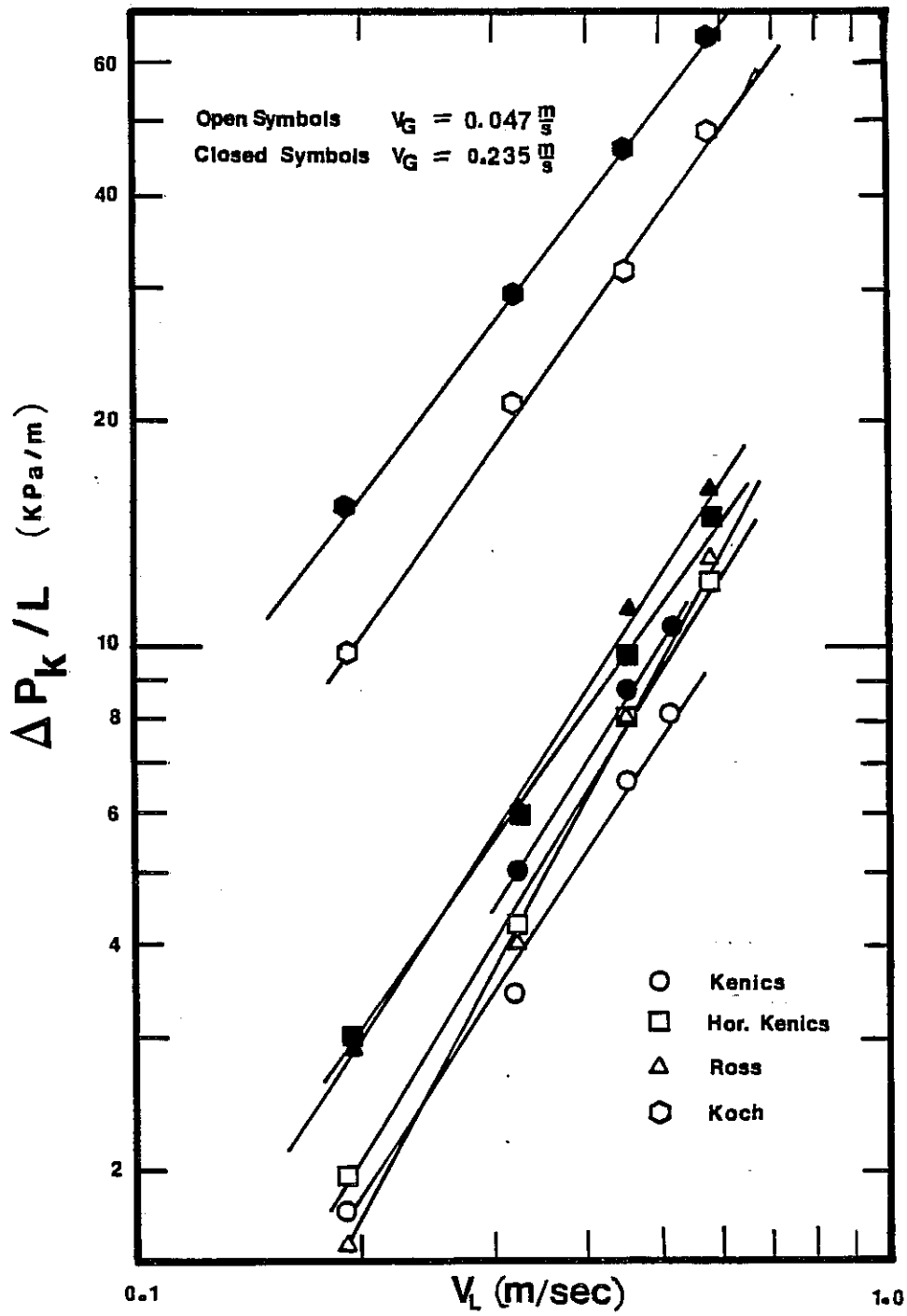

Figure 17. Effect of Fluid Velocities on Pressure Drop Per Unit Length for All Mixers

Kenics, Koch, Ross mixers at a high and low gas velocity for a nitrogen/water system.

Although an in depth analysis of the pressure drop data of this experiment is beyond the scope of this paper, some general comments can be made. 1) The Koch mixer has a significantly higher pressure drop than the other two mixers. 2) The kinetic pressure drop is slightly greater for horizontal flow than vertical flow in the Kenics mixer. 3) The slopes of the constant gas velocity lines are around 1.5 and less than 2.0 which is predicted from the homogeneous model. These slopes are affected by the change in gas velocity but only slightly. 4) By increasing this the superficial gas velocity, the kinetic pressure drop is increased. This phenomenon was also discovered by Smith in his paper (2).

4.3 INTERFACIAL AREA AND MASS TRANSFER COEFFICIENT

Before the results of these experiments can be presented some assumptions and corrections needed to be devised to compensate for some problems that arose during the experimentation. These two corrections are the separator/sparger correction and the correction to compensate for the uptake of the pure carbon dioxide gas.

4.3.1 Separator and Sparger Correction

Since the separator had a significant volume compared to the volume of the reactor, some mass transfer occured in the separator. Also, the initial creation of interfacial

area at the gas inlet, which is not a result of the mixer, has some associated mass transfer. These two effects were orginally assumed to be significantly less than in the reactor since the gas bubbles should be coalescing in the separator and the actual volume around the sparger is small. However, by bypassing the reactor and sparging the gas just below the entrance to the separator at the top pressure tap location and measuring the rate of absorption, it was determined that the absorption from these two effects were significant. Unfortunately, these two effects were experimentally inseparable and could only be measured together.

Appendix 7.5 gives the details of the results of those experiments, their interpretation and the derivation of some correction schemes. Briefly those results showed that the effect of the separator and sparger can be approximated by extending the defined volume of the reactor by the same amount as the product of the distance between the top of the reactor and the liquid level in the separator and cross sectional area of the tubular reactor. In other words, the total reactor volume includes the volume of the 0.0254 m diameter cylinder down the center of the separator. Visually, the bubbles maintain their integrity and do not spread radially as they pass through the separator to the liquid surface. So this approximation also makes practical sense.

4.3.2 Gas Phase Depletion Correction

Since the gas used was pure carbon dioxide, the molar flowrate of the gas stream constantly decreased with increasing distance up the reactor. As the gas was absorbed, the interfacial area also decreased. One possible solution could have been to label the interfacial surface area experimentally determined as an average area for the mean of the inlet and outlet gas flowrate. Unfortunately, this simple minded approach fails because of the way that the interfacial area is evaluated. The interfacial area is extracted from the slope of a line comprised of experimental points evaluated at different catalyst concentrations. Since the rate of absorption is different at each catalyst concentration, the outlet gas flowrate, and thereby the average gas flowrate, would be different for each point.

Appendix 7.6 shows the development of a correction scheme to correct the measured rate of absorption to account for the changing molar gas rate. Once the rate of absorption is corrected for each catalyst concentration then those points are plotted as originally planned.

Figure 18 shows the original data and correlating straight lines based on the volume of the physical reactor (line A). It also shows the subsequent effect of the separator and sparger correction (line B) and finally the effect of the gas depletion correction scheme (line C). Table 3 shows the resulting interfacial area, a, and mass transfer coefficient, k_L, that are calculated from the

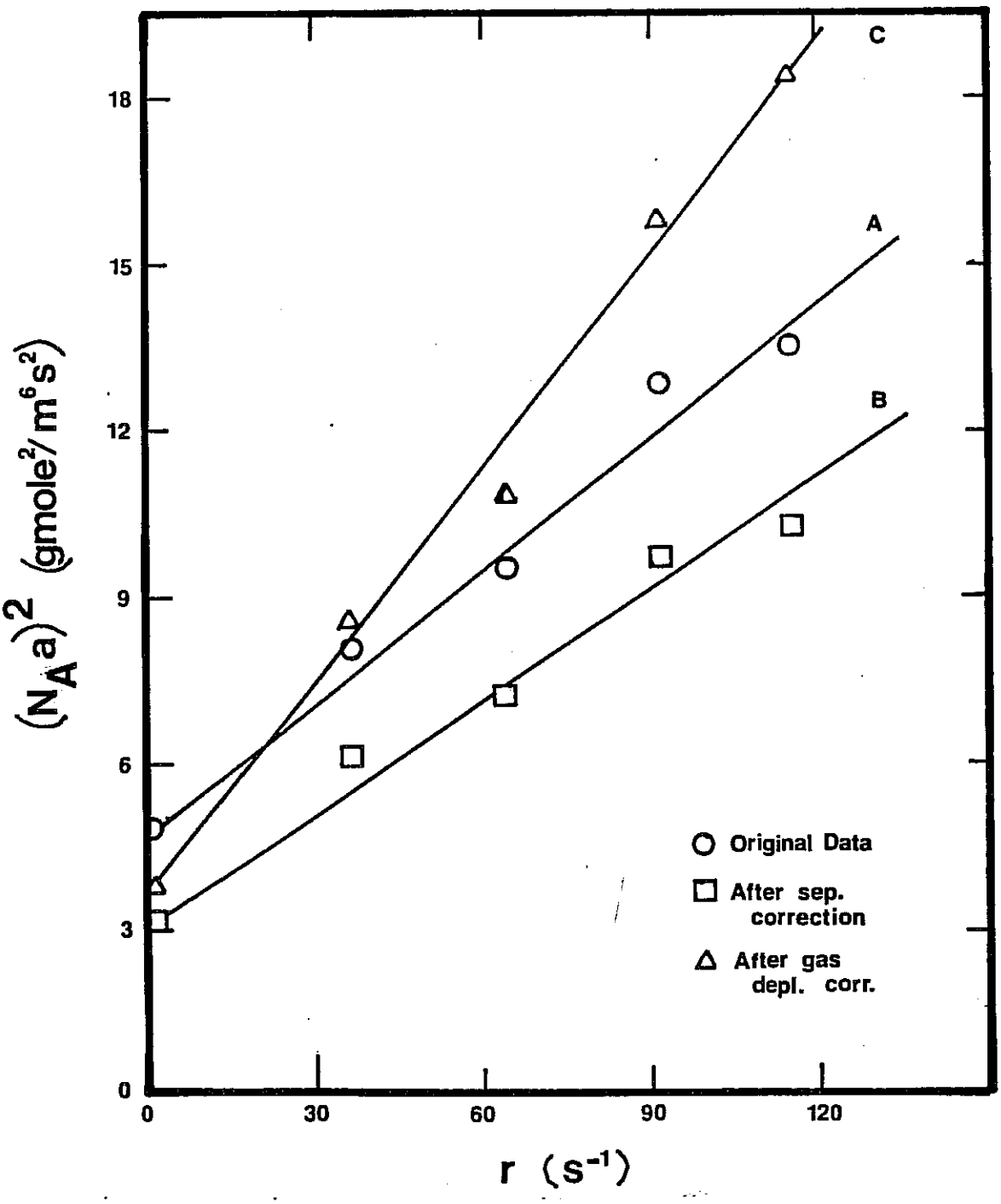

Figure 18. Effect of the Correction Schemes on the Danckwerts' Plot

Table 3

Effect of Correction Factors on the Experimental Values of the Mass Transfer Coefficient and Interfacial Area

Line	Intercept	Slope	a	k_L
	$mole^2/m^6 s^2$	$mole^2/m^6 s$ x 10^2	m^{-1}	m/s x 10^4
A	4.6	8.15	371	2.8
B	3.1	7.36	352	2.4
C	3.4	13.7	472	1.8

slopes and intercepts of each of the lines. In review, a and k_L are calculated from the following equations:

$$a = \frac{\sqrt{\text{slope}}}{C_{A_i}\sqrt{D_A}} \tag{36}$$

$$k_L = \sqrt{D_A\left(\frac{\text{intercept}}{\text{slope}}\right)} \tag{37}$$

The gas depletion in the Koch mixer was extreme, such that the "correction" became more significant than the actual measured rate of absorption. In fact, at medium and high catalyst concentrations the gas was almost completely absorbed. Therefore, it became impractical with the current experimental apparatus and procedure to obtain a Danckwerts' plot in order to evaluate a and k_L separately in this mixer. However, it was still practical to measure the rate of absorption with no arsenite and to evaluate k_La by the following formula:

$$N_A a = k_L a\, C_{A_i} \tag{20}$$

So k_La can be measured experimentally and a can be evaluated from the assumption that k_L in the Koch mixer is equal to the k_L that was experimentally measured in the Kenics and Ross mixers. The foundations for this assumption will be supplied in the following sections.

4.3.3 True Mass Transfer Coefficient

Based on the experimental results for the Kenics and Ross mixers, the true mass transfer coefficient, k_L, was found to be constant within experimental error for the gas and liquid flowrates studied. These results are presented in Table 4. The average value for k_L is 1.84×10^{-4} m/s with a standard deviation of 0.27×10^{-4} m/s. Also included in Table 4 are the predicted values of k_L from equation (6) from experimental values of d_B and ΔV. Comparison shows that the predicted values for k_L are up to 10 times larger than the experimental values and also that the predicted values vary with the flow conditions while the experimental values are essentially constant.

This analysis shows that the flow conditions and turbulence in the experimental system do not match the conditions for which equation (6) was derived. It also casts doubt on any proposed method using this equation to predict values of k_L or k_La for static mixers in a vertical configuration, i.e. the method described in Section 1.3 by Holmes and Chen.

Interestingly, the situation for which equation (6) was derived is less turbulent than the situation from which the experimental values were determined and yet the experimental mass transfer coefficients are smaller. This result as well as the constancy of k_L with changes in bubble diameter is verified by Figure 19; a plot presented by Calderbank and

Table 4

Comparison of Experimentally Determined Mass Transfer Coefficients and Values Predicted by Equation (6)

V_L	V_G	$1-\epsilon$	ΔV	d_B	eq. (6) k_L	exp. k_L
m/s	m/s		m/s	m	m/s	m/s
				$x10^4$	$x10^4$	$x10^4$
0.630	0.146	0.93	1.41	3.13	28.1	1.64
0.450	0.146	0.90	0.96	7.96	14.6	1.81
0.193	0.146	0.88	1.00	18.27	9.8	1.92
0.450	0.219	0.87	1.17	7.58	16.5	1.70
0.450	0.073	0.95	0.99	6.20	16.7	2.13
0.630	0.146	0.93	1.41	5.41	21.4	2.28
0.450	0.146	0.91	1.13	11.23	13.3	1.85
0.193	0.146	0.85	0.746	31.58	6.4	1.83

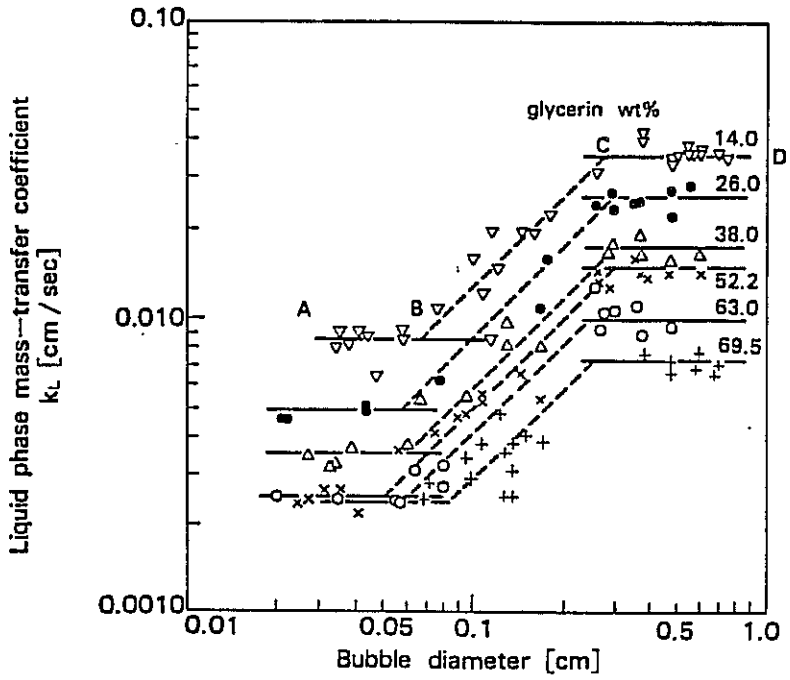

Figure 19. Effect of Bubble Diameter on the Mass Transfer Coefficient (25)

Moo-Young for carbon dioxide absorption into various glycerin solutions at 25°C in agitated vessels (25).

The abscissa of Figure 19 is the bubble diameter which is indirectly related to the turbulence created by the impeller. The figure shows that k_L goes through a decreasing transition range as the turbulence is increased. It also shows that at either end of the transition range, k_L remains constant. Most of the results of this study fall in the high turbulence range. Therefore a constant experimental value of k_L is comprehendable.

Since the degree of turbulence is higher (the bubble diameter is smaller) in the Koch mixer and the experimental k_L for the Kenics and Ross mixers was constant, then the assumption that k_L would be the same in the Koch mixer seems reasonable for the same fluids.

Wang and Fan (8) in their study of mass transfer in bubble columns filled with AY Koch mixers, suggest that:

$$k_L \propto V_L^{0.733} V_G^{0.01} \tag{38}$$

This finding definitely contradicts the above statement. Their conclusion is based on experimental correlations of k_La and ϵ given below:

$$k_La = C_1 V_L^{0.631} V_G^{0.589} \tag{3}$$

$$\epsilon = C_2 V_L^{-0.102} V_G^{0.588} \tag{4}$$

Equation (38) was derived on values of holdup correlated by equation (4), values of volumetric mass transfer coefficient correlated by equation (3), and on the assumption that area, a, is proportional to gas holdup, ϵ. Unfortunately they seemed to have missed one point. From equation (6) a is proportional to ϵ, but it is also inversely proportional to d_B, which is also a function of flowrates. The equation developed by Streiff for d_B can be written in the crude form:

$$d_B = C_3 \, V_L^{-0.85} \tag{39}$$

Since

$$a = \frac{6 \, \epsilon}{d_B} \tag{6}$$

then

$$a = C_4 \, V_L^{0.748} \, V_G^{0.588} \tag{40}$$

and therfore from (3) and (40)

$$k_L \propto V_L^{-0.117} \, V_G^{0.001} \tag{41}$$

This is now a more reasonable correlation for k_L, showing that it is a very weak function of flow conditions and showing an overall weak decrease as the turbulence, caused by increased liquid velocity.

Mangartz and Pilhofer (26) studied mass transfer coefficients in bubble columns with a similar system; air/water/carbon dioxide. They compared their results with a few correlations. These correlations are as follows:

Calderbank and Moo-Young (25)

$$k_L = 0.31 \left[\frac{\rho_L D_A}{\mu_L}\right]^{2/3} \left[\frac{(\rho_L - \rho_G)\mu_L g}{\rho_L}\right]^{1/3} \quad d_B < 2.5\text{mm} \qquad (42)$$

$$k_L = 0.42 \left[\frac{\rho_L D_A}{\mu_L}\right]^{1/2} \left[\frac{(\rho_L - \rho_G)\mu_L g}{\rho_L}\right]^{1/3} \quad d_B > 2.5\text{mm} \qquad (43)$$

Hughmark (27)

$$\frac{k_L d_B}{D_A} = 2 + 0.0187 \left[\left(\frac{d_B \Delta V}{\mu_L}\right)^{0.484} \left(\frac{\mu_L}{D_A}\right)^{0.339} \left(\frac{d_B g^{1/3}}{D_A^{2/3}}\right)^{0.072}\right]^{1.61} \qquad (44)$$

and Higbie (28)

$$k_L = 1.31\sqrt{\frac{D_A \Delta V}{d_B}} \qquad (6)$$

Of these three correlations, they found that the correlation by Calderbank and Moo-Young provided the best fit. Their measured k_L value was about constant for various gas and liquid rates and averaged around 1.0×10^{-4} m/s.

This study's value for k_L, 1.84×10^{-4} m/s is approximately 80% higher than their value. This discrepancy can be partly explained by the effect of a chemical reaction on k_L. Linek (15) in his comprehensive article mentions an experiment done using oxygen and argon as different

absorbing gases into sulphite solution with no catalyst. The argon absorption is a physical process while the oxygen absorption is chemically enhanced. Linek found that the oxygen transfer coefficients were about 50% higher than those of argon.

4.3.4 Interfacial Surface Area

This section is concerned with how experimental values of a and $k_L a$ are affected by the changes in superficial velocities. The next section will show the functional dependence of these experimental values on dissipatated power.

Figures 20 and 21 present interfacial area, a, versus V_L and versus V_G respectively for each reactor type. From these plots the following correlations were developed:

Kenics $$a \propto V_L^{1.0} V_G^{0.68} \quad (45)$$

Ross LLPD $$a \propto V_L^{0.85} V_G^{0.68} \quad (46)$$

Koch CY $$a \propto V_L^{0.67} V_G^{0.89} \quad (47)$$

The effect of V_G on area, a, in the Ross mixer was not evaluated, but it can be assumed to be similar to the Kenics mixer. The exponents for the Koch mixers are averaged from the different slopes on each plot.

The ordinate on the right hand side, which is accompanied by the closed symbols, refers to a redefinition of

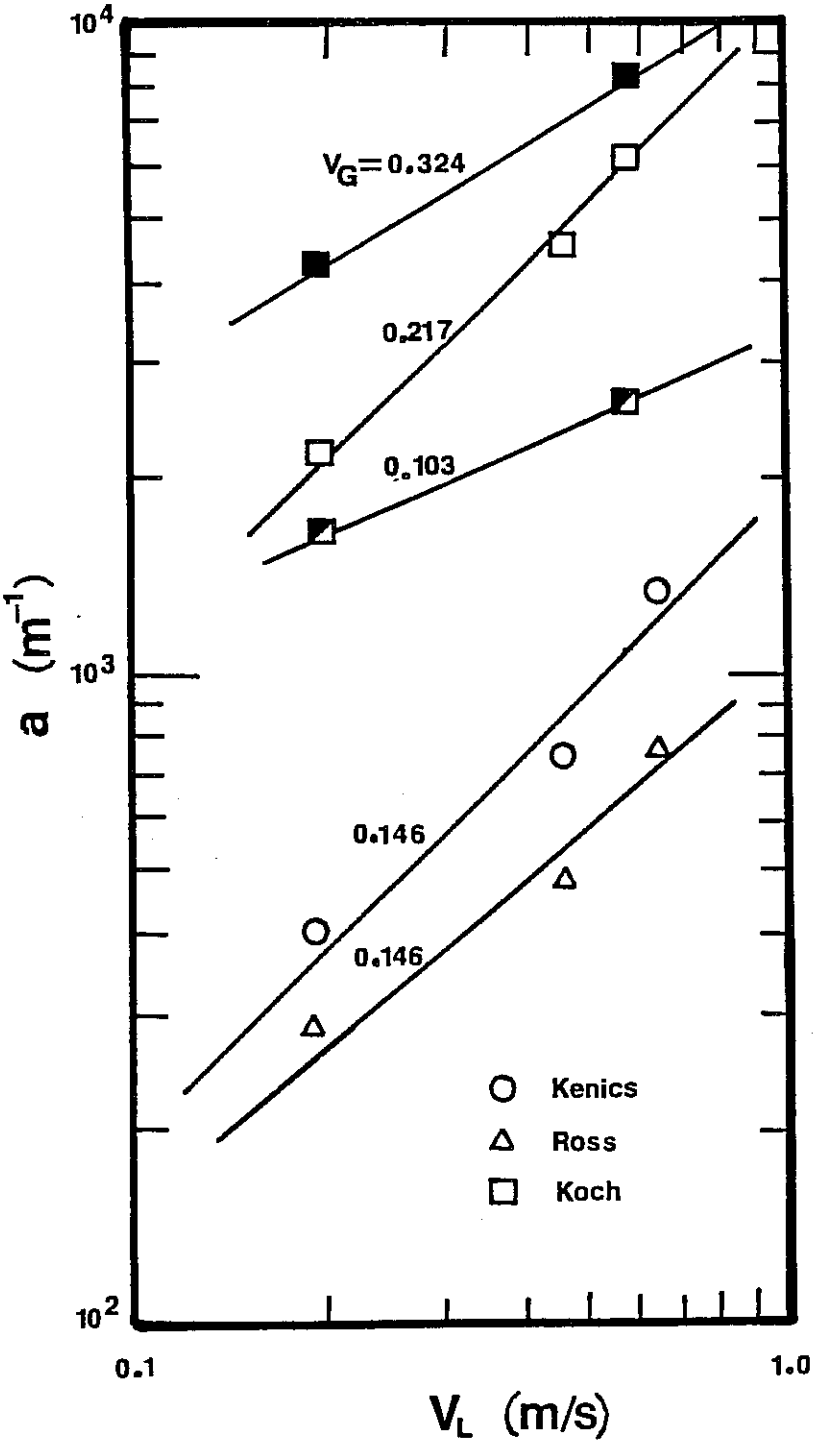

Figure 20. Effect of Liquid Velocity on Interfacial Area for All Mixers

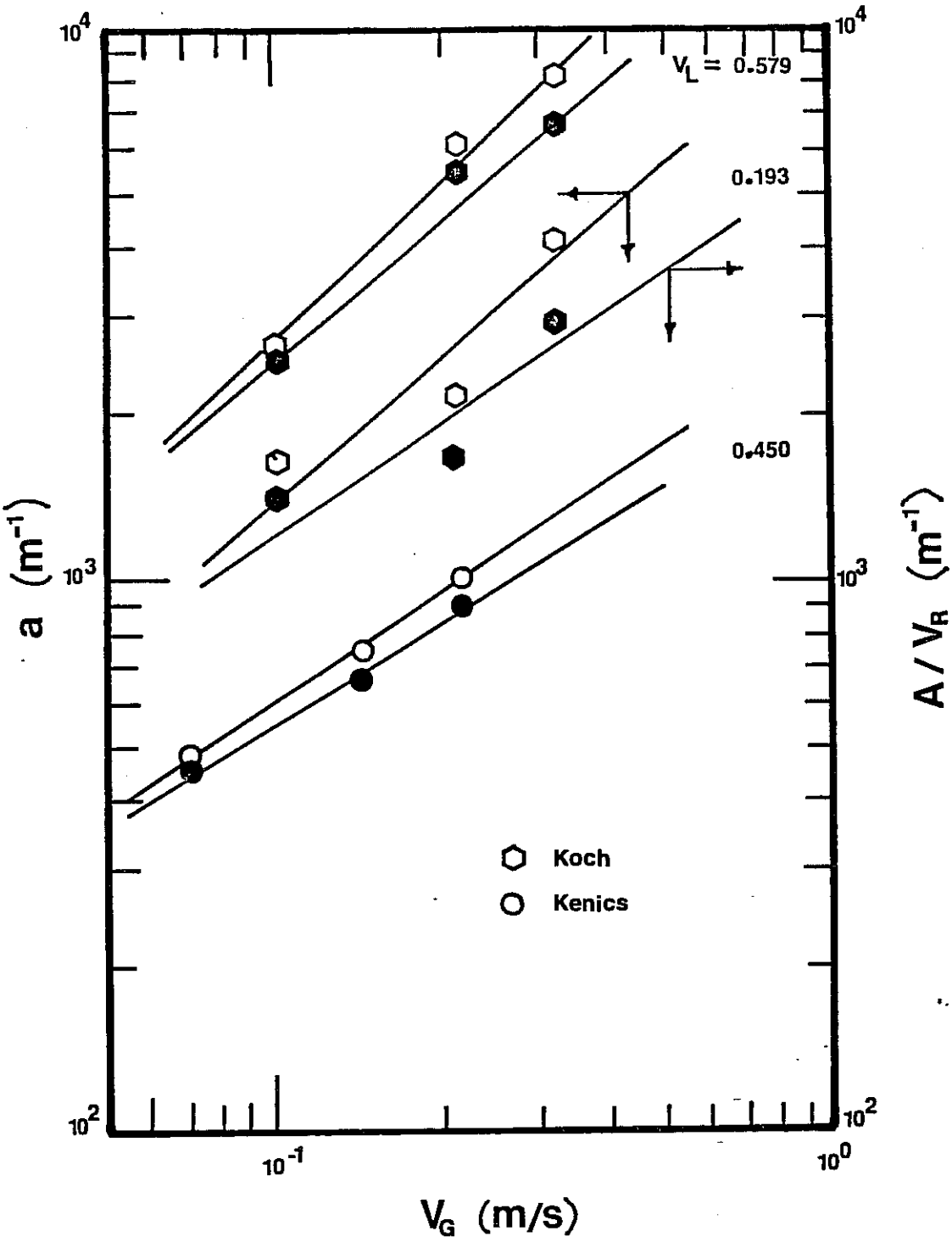

Figure 21. Effect of Gas Velocity on Interfacial Area for the Kenics and Koch Mixers

the interfacial surface area by using a basis of volume of both phases instead of volume of liquid only. This will be used in the next section.

Generally, for the same gas and liquid superficial velocities, the Kenics mixers slightly out perform the Ross LLPD mixers while the Koch CY mixer with spacers provides approximately 4 times the amount of interfacial area per unit liquid volume.

4.4 Efficiency of Static Mixers

The efficiency of a gas/liquid contactor can be found by determining the amount of interfacial area for a given dissipated power. By plotting values of interfacial area per unit volume of liquid, a, versus the dissipated power per unit liquid volume, P_w, for different gas/liquid contactors on the same figure, the efficiency of the different contactors can be compared.

Figure 22 is an efficiency plot for the results of this study for the three different static mixers. This figure shows that the Ross LLPD mixer is the least efficient and that the CY Koch mixer with spacers is the most efficient. The Koch mixer can produce up to 3 times more interfacial area for the same power input that the Kenics mixer.

One desired result of this study is to compare these efficiencies to other gas/liquid contactors. Nagel et al. (29, 30) have done studies of interfacial area in various gas/liquid contactors and presented the results for one gas

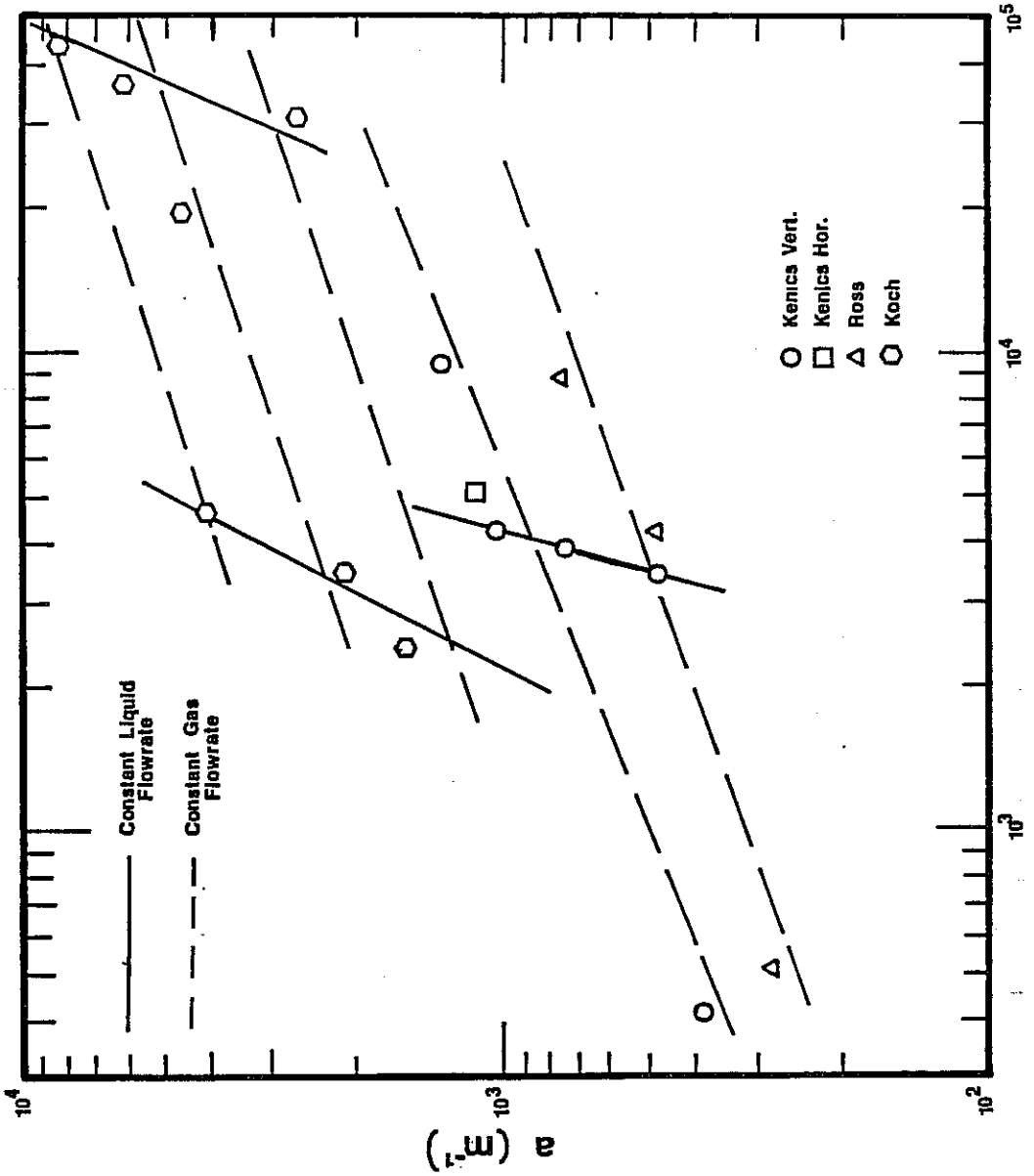

Figure 22. Comparative Efficiencies of the Static Mixers at Various Flow Conditions

flowrate versus power dissipation. Before this data is presented, some details need to be addressed.

First, Nagel's interfacial areas were also determined by a chemical method, only the chemical reaction used was the absorption of oxygen into sulphite solution. Although, his results are for a different chemical systems, Alper (31) showed experimentally that the two chemical systems (carbon dioxide absorption into carbonate/bicarbonate buffer solution with an arsenite catalyst and oxygen absorption into sulphite solution with a cobalt catalyst) give essentially the same interfacial areas.

Second, Nagel defines his interfacial area and power dissipation per unit two phase volume instead of volume of the liquid only. So all the subsequent results needed to be multiplied by the appropriate liquid holdup values.

Finally, Nagel's data is only for one gas flowrate of 0.047 m/s and undetermined liquid flowrates. Unfortunately this particular gas velocity was impratical to perform experimentally in the static mixers. Therefore, since it is apparent from Figure 22 that the gas rate does affect the efficiency of the mixers significantly, this study's results need to be adjusted to this lower gas rate before a comparison could be made.

Nagel (29) does suggest a correlation to account for the effect of the gas rate. In this study's terminology this correlation becomes:

$$\frac{A}{V_R} = C_5 \left(\frac{E}{V_R}\right)^m V_G^n \tag{48}$$

where $\frac{A}{V_R}$ = Interfacial area per unit reactor voidage, (m^{-1}); and

$\frac{E}{V_R}$ = Power dissipation per unit reactor voidage, (W/m^3).

Plotting $((A/V_R) \cdot V_G^{-n})$ versus (E/V_R) should create a single line instead of a family of lines. The exponent on the gas velocity for the static mixer are from the previous sections analysis. Figure 23 is such a plot with each reactor. From this plot C_5 and m are calculated and the final correlations are as follows:

Kenics $$\frac{A}{V_R} = 77 \left(\frac{E}{V_R}\right)^{0.42} (V_G)^{0.59} \tag{49}$$

Ross LLPD $$\frac{A}{V_R} = 34 \left(\frac{E}{V_R}\right)^{0.48} (V_G)^{0.59} \tag{50}$$

Koch CY $$\frac{A}{V_R} = 344 \left(\frac{E}{V_R}\right)^{0.37} (V_G)^{0.76} \tag{51}$$

Now that these correlations have been developed it is easy to backtrack and calculate interfacial areas at the gas velocity of 0.047 m/s for various power inputs and then plot

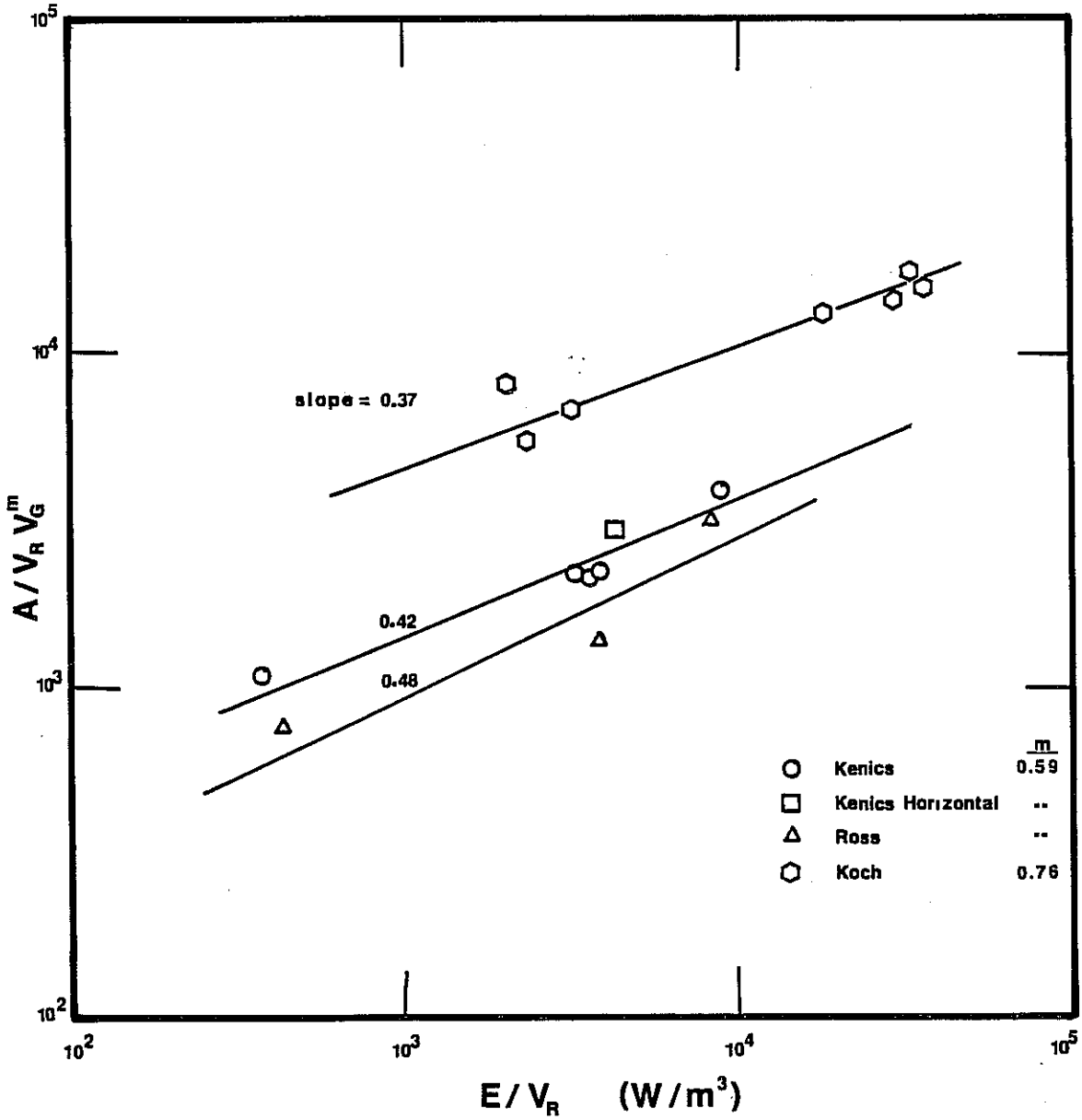

Figure 23. Efficiencies of the Static Mixers that Account for Variable Gas Flowrates

these values on Nagel's diagram (30). This was done and the final result is Figure 24. This figure shows that only the Koch mixer is competitive to the other gas/liquid contactors.

Although this plot is only valid for one gas flowrate, its validity could be extended to all gas flowrates if the other contactors have roughly the same relationship between the interfacial area and gas flowrate. This point is important since it is not recommended to operate static mixers at this gas flowrate, whereas the other devices may be well suited for this low gas rate. Refering to equation 48, the exponent n equals 0.5 and 0.7 for the packed and bubble columns, respectively (32), but less than 0.5 for a stirred tank (33). So Figure 24 would be an adequate representation of the comparative efficiences for the static mixers and the packed and unpacked bubble columns. Depending on the exact value of n for stirred tanks, the static mixers' efficiencies may become more comparable to stirred tanks at higher gas flowrates.

From the equations 49 through 51, the exponents of the power dissipation for the static mixers are around 0.4. This is the same as the exponent for packed columns and two-phase vertical and horizontal flows in empty pipes. It also corresponds to the theoretical value of 0.4 from Kolmogoroff's theory of area production (29). However, stirred tanks have a much higher exponent than these other mixers which has been shown to be of the order of 0.8.

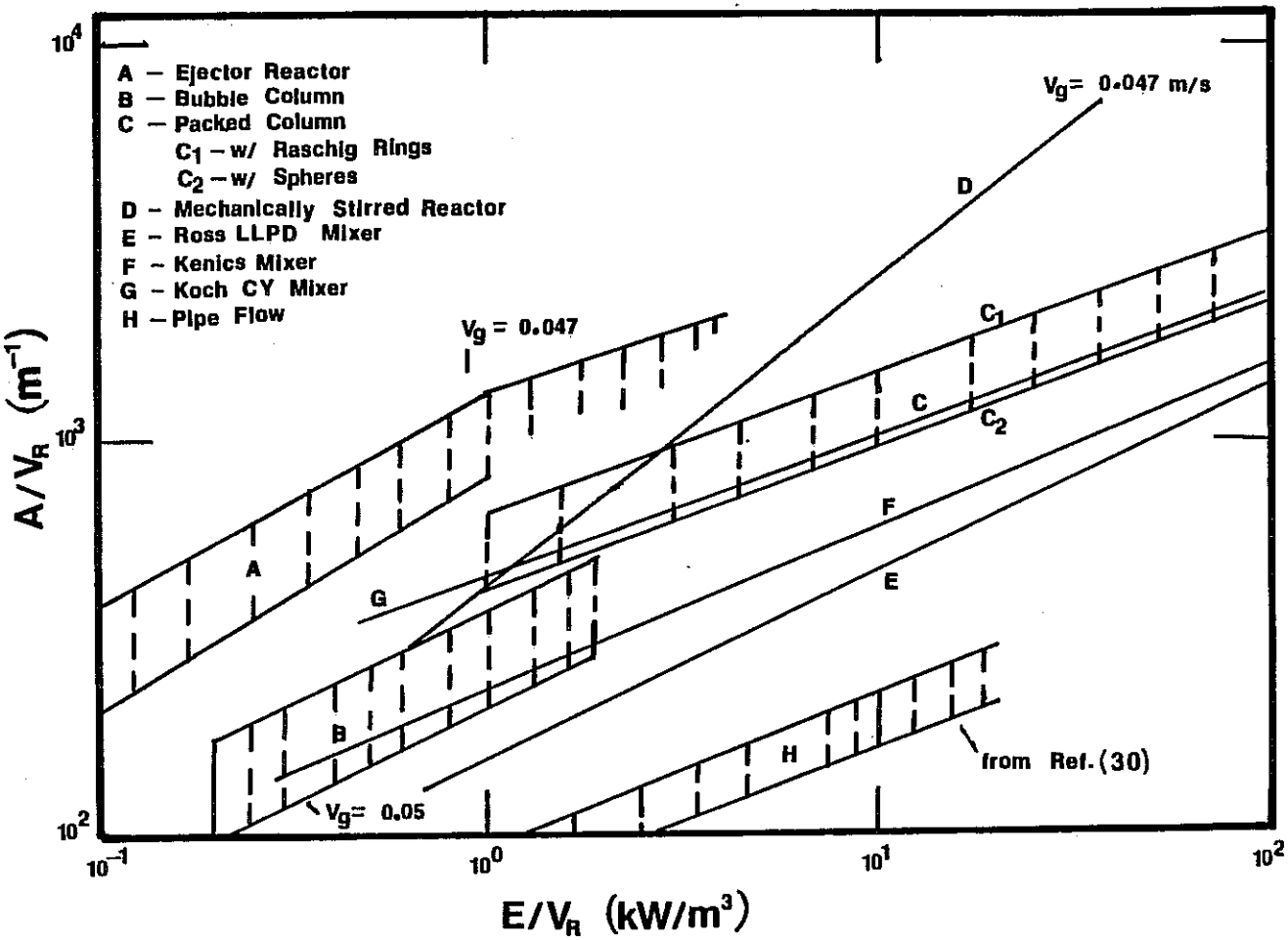

Figure 24. The Efficiencies of the Static Mixers Compared with Other Gas/Liquid Contacting Devices at One Gas Velocity

Middleton (3) reports that from k_La measurements that the exponent to which dissipated power is raised for all gas/liquid contactors including static mixers is 0.8. From the assumption that k_La and a differ only by the constant factor of k_L (providing that the power input is high enough to be past the transition range) this is equivalent to claiming that the interfacial area is proportional to the rate of energy dissipation raised to a power of 0.8. Middleton (3) arrives at that conclusion based on his interim experimental results of k_La values in gas/liquid upflow for empty tubes and tubes containing meshes, Kenics mixers, Sulzer (Koch) mixers, and Etoflo mixers.

Figure 25 is his figure for interfacial area versus power dissipation including only his Kenics and Sulzer (Koch) mixer results. Line A is the line plotted by Middleton through all his data based on which his conclusion is formulated. The raw data is unquestionable but the analysis seems incorrect. In light of this study it would seem more appropriate to construct two separate lines; one line correlating the Sulzer (Koch) data (line C) and one line passing through the Kenics data (line B). If this is done, the exponents for the dissipated power are 0.48 for the Kenics mixer and 0.47 for the Sulzer (Koch) mixers which are more consistant with the findings of this study.

No information about which type of Sulzer (Koch) mixer was used, nor about the specific gas and liquid rates was reported by Middleton. However, the data of this study

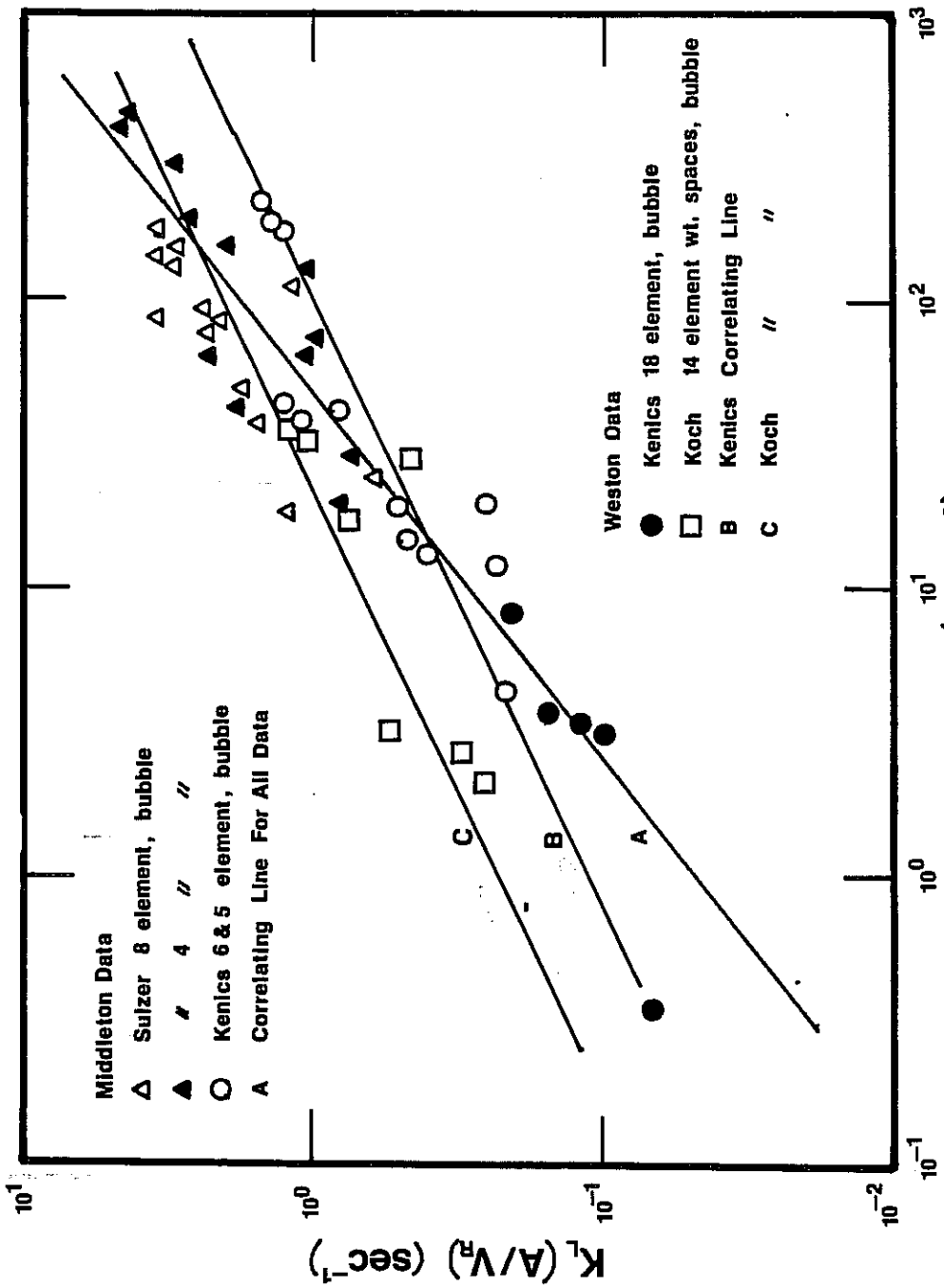

Figure 25. Interfacial Area versus Power Dissipation Containing This Study's Results and Middleton's Results (3)

plotted on Figure 25 seems to correlate well with Middleton's results and to extend them to a broader range.

4.5 COMMENTS

4.5.1 Spacing

The reason for spacing the Koch CY mixers in the pipe was an attempt to get the same reactor length. Since Wang and Fan found that the use of spacers did not significantly reduce the mass transfer, and since it did reduce the pressure drop across the reactor, it made sense to use the spacers. It may even be the only reason why the Koch mixer was as efficient as it was found to be.

This does raise an interesting question. If the same reactor was used, but the spacers were doubled in length, would the reactor be more efficient? Unfortunately, no studies were done specifically to answer this question. However it seems logical that there should be an optimal spacing to maximize the efficiency of the reactor which may occur when the average time required for to bubbles to coelesce equals the travel time of a fluid element containing those two bubbles to travel between two mixer elements.

Since the Kenics mixers are more efficient than an empty pipe, it also raises the possibility that a combination of Koch and Kenics mixers, where the Kenics mixer replaces the spacer, might be a very efficient mixer.

4.5.2 Horizontal Mixers

This study was basically involved with static mixers in a vertical position. The reason for doing the experiments

in that configuration was that the holdup measurements were easier to accomplish and that there was positively no layer separation.

Since industrial users potentially are more interested in these mixers in a horizontal configuration, one absorption run was done in a horizontal Kenics mixer. The results showed that the horizontal mixer was just as efficient as the vertical mixer. In fact, the amount of interfacial area created was greater than that in a vertical mixer. The reason for this is because of the larger gas holdup in the horizontal reactor. From the holdup measurements, the horizontal mixer always has a larger holdup. Therefore, it is reasonable to assume that for nearly all flow conditions, the amount of interfacial area produced in a horizontal reactor will be greater than in the vertical reactor.

4.5.3 Chemical Method Usefulness

One of the underlying goals of the project was to test the usefulness of the carbon dioxide absorption chemical method for the determination of k_L and a separately. Also, another equally important purpose was to develop or refine the titration methods necessary to properly measure the amount of absorption. Some overall comments, more than just an error analysis, need to be presented.

The liquid side evaluation of absorption through titrations should be avoided if possible. If the measurements can be accomplished on the gas side either by

flowrate measurements or gas chromatography without causing experimental difficulties such as excessive pressure requirements or sophisticated sampling equipements then this should be prefered. This statement arises form the complexity, heavy time requirements and significant errors of the titrations.

If gas side measurement is definitely not feasible, then to reduce the time and error of the titrations, the experimentor should try to operate at low concentrations of the catalyst. The reduced concentration of the arsenite makes the titrations more accurate and somewhat easier.

Dr. Ashok Gokarn (34) is currently working on a project in which gas side measurements are impractical and is therefore utilizing the titration methods developed by this study. He is using catalyst concentrations up to 0.25 M and his preliminary comments suggest that the method is useful and the results from the experiments are satisfactory.

If the experimenter needs to use high concentrations of the catalyst for any reason (i.e. higher rates of absoption or higher Hatta numbers) then another system like oxygen absorption into sulphite solution using a cobalt catalyst should be seriously considered.

Concerning the usefulness of measuring k_L and a separately, it should be mentioned that since k_L was found to be a constant, a definite value for k_L was measured and it seems to be reasonable with respect to what is currently reported in the literature. Since k_L is a parameter that is

very dependent on a particular chemical system, it is valuable to experimentally determine a value for it.

When a value for k_L is obtained it is no longer necessary to measure area, a from a Danckwerts' plot. All that is required is to measure k_La and divide by the known value of k_L. The measurement of k_La and the subsequent titrations are an order of magnitude easier and more accurate, since this measurement relies on the titration of the solution with no arsenite. Remember that the although the buffer solution does not contain arsenite the absorption is still chemically enhanced and the k_L measured from the Danckwerts' plot is the appropriate value.

If future experiments were to be done regarding the optimal Koch mixer spacing, only k_La needs to be determined, as long as the same solution (i.e. concentrations and ionic strengths) were used.

4.5.4 Error Analysis

A simple minded error analysis was done on the calculated values of the interfacial surface area and mass transfer coefficient. The major error in the analysis was brought about by the titration errors. All other measurement errors were significantly smaller.

Each titration to determine the bicarbonate concentration before and after a run was done at least three times. From those three values an average and an error was calculated. Since the change in concentration was

the desired result, the subtraction was made and the errors added. From this, a percentage error was calculated.

One set of flow conditions was repeated once for various arsenite concentrations and the resulting deviations were within the titration error. The experimental procedure of dilution was tested also by repeating a zero catalyst concentration run at a single flow condition four times. The results were all within titration error.

After the gas correction was taken and the resulting values of ($N_A a$) were plotted on a Danckwerts' plot, the percentage errors (now doubled because of the square) were also plotted as error bars. A sample plot is given in Appendix 7.7. Then three lines were drawn , one of high slope, one of low slope and the best eye reckoned slope through the points and error bars. From the deviations of the resulting values of a and k_L, a new percentage error was determined.

The run that was selected to present this error analysis in Appendix 7.7 was an early run when the errors were very large. Therefore this analysis should give a maximum error.

The error in the values of area, a are 15% and for k_L are 31%. In the case of the Koch mixer where no Danckwerts' plots were used the error of area, a, was equal to the titration errors which were no more than 10%.

4.5.5 Hatta Numbers

For the results to have meaning, the conditions as specified by the derivation in Appendix 7.8 for the Hatta number and the instantaneous enhancement factor must be satisfied. The Hatta numbers, depending on the catalyst concentrations, ranged from 0.3 to 2.8. The instantaneous enhancement factor was calculated and was equal to 21. So the condition:

$$E_i /2 \gg Ha \qquad (52)$$

was satisfied. However, the suggested requirement (15) on the Hatta number:

$$Ha \gg 3 \qquad (53)$$

was not satisfied. This is not as debilitating as it may seem at first sight. Appendix 7.8 is an analysis on the effect of low Hatta numbers on the enhancement factor. It is shown that the first criterion, equation (52), must be satisfied but that the second one, equation (53), may be unnecessary.

This analysis also shows that for all but the zero concentration points, the error due to low Hatta numbers is less than 1%. For the zero catalyst concentration points the error is less than the titration errors.